Stable Simple Enols. 3.[1] Static and Dynamic NMR Behavior of Crowded Triarylethenols and Related Compounds. Three-Ring Flip as the Threshold Mechanism for Enantiomerization of Crowded Triarylvinyl Propellers

Silvio E. Biali and Zvi Rappoport*

Contribution from the Department of Organic Chemistry, The Hebrew University of Jerusalem, Jerusalem 91904, Israel. *Received April 4, 1983*

Abstract: The static and dynamic stereochemistry of vinyl propellers $Ar^3Ar^2C{=}C(X)Ar^1$ (**2**) was analyzed and compared with those for the $Ar^1Ar^2Ar^3Z$ (**3**) and $Ar^1Ar^2Ar^3ZX$ (**4**) molecular propellers. The number of the maximum labeled propellers for each configuration of **2** is smaller than for **4**, but permutations leading to positional and *E*,*Z* isomers of **2** increase the overall number when $Ar^1 \neq Ar^2 \neq Ar^3$. Five possible stereoisomerization routes were analyzed: (i) rotations around the C(sp²)–C(Ar) bonds including various types of "flip" mechanisms; (ii) rotation around the double bond; (iii) addition–rotation–elimination; (iv) ketonization–enolization; (v) ionization–recombination with or without β-aryl rearrangement across the double bond. The DNMR behavior of several triarylvinyl propellers, which exist only as a pair of (helicity) enantiomers since the three rings have local C_2 symmetry, was investigated. Trimesitylethenol ($Mes_2C{=}C(OH)Mes$, **1**) shows at room temperature 16 separate singlets in the ^1H NMR spectrum, one each for the methyl groups, the aromatic protons, and the OH, in line with a propeller conformation in solution. By use of analogues with α- and β-2,4,6-$(CD_3)_3C_6H_2$, α-2,6-$Me_2C_6H_3$, and β-4-*t*-Bu-2,6-$Me_2C_6H_2$ rings and by application of aromatic-solvent-induced shifts, off-resonance, and saturation transfer techniques, all the ^1H NMR signals and most of the ^{13}C NMR signals were identified. A ^1H dynamic NMR study of the coalescence of the three pairs of methyl protons and one pair of aromatic protons and a ^{13}C DNMR study of one pair of aromatic carbons were conducted in $C_6D_5NO_2$ and identical $\Delta G_c^{\ddagger}$ values (18.4 ± 0.1 kcal mol^{-1}) were found for the three rings. These values are nearly independent of the solvent and insensitive to addition of CF_3COOH. Analysis of the enantiomerization routes suggested that the process followed is a correlated rotation involving a three-ring flip. This is the mechanism for the enantiomerization as shown by the identical $\Delta G_c^{\ddagger}$ values for the three rings and for the isopropyl doublets of trimesitylvinyl isopropyl ether (**19**), where the isopropyl group serves as an enantiomerization probe. The case for a three-ring flip is strengthened by the identical $\Delta G_c^{\ddagger}$ values of the three rings of 1-(9-anthryl)-2,2-dimesitylethenol (**25**). The $\Delta G_c^{\ddagger}$ values for $Mes_2C{=}C(X)Mes$ are 18.4, 19.0, 15.8, and 16.4 kcal mol^{-1} when X = OH (**1**), OAc (**18**), $OCHMe_2$ (**19**), and Cl (**20**), respectively, and 16.2 for **25**. The lower barrier for **25** is ascribed to a higher torsional angle of the α-ring in the ground state, as verified by X-ray diffraction of solid **25** and to a lower transition-state energy since a mesityl group is wider than an anthryl group. X-ray diffraction data for **18** indicate a propeller conformation. The low-temperature ^1H NMR of **1** and **19** shows only one signal for X, but that of **18** at 212 K shows a 3.4:1 ratio of two conformers due to a different orientation of the acetate group. The $\Delta G_c^{\ddagger}$ for their interconversion is 12.1 ± 0.3 kcal mol^{-1}, and possible stereoisomerization routes were suggested. Structural requirements for the preparation of conformationally stable optically active vinyl propellers were discussed.

The kinetics and equilibria of keto ⇌ enol tautomerism have been a main topic of research in physical organic chemistry for a long time.[2] "Simple" enols (i.e., those substituted by hydrogen, alkyl, and/or aryl groups) were usually regarded as kinetically or thermodynamically unstable, and studies of their reactions or of the keto ⇌ enol equilibria were based on an indirect measure of their reactivity and concentration.[2-4] However, as summarized by Hart[5] there are a fair number of simple enols of moderate stability, and even vinyl alcohol itself, the simplest member of the class,[6] and related enols[7] were prepared recently in solution[6,7] or in the gas phase[8] as species with sufficiently long lifetimes for kinetic and spectroscopic investigations, in spite of their low thermodynamic stabilities.

In contrast, a series of kinetically stable (i.e., isolable) simple sterically hindered diaryl- and triaryl-substituted enols has been prepared many years ago by Fuson and co-workers. In some cases the enols were even more stable than the keto forms.[9] Surprisingly, these enols were almost completely neglected by most textbooks and reviews,[10] and very little mechanistic study was conducted with them and with related compounds.[11] The present work is a part of an extensive study directed toward delineating the reasons for the stabilities of the enols, their properties, and their reactions in the gas phase[12] and in solution.[1] The high crowding, which is at least partly responsible for this stability and

(1) (a) For a preliminary communication, see: Biali, S. E.; Rappoport, Z. *J. Am. Chem. Soc.* **1981**, *103*, 7350. (b) For other reactions of stable enols in solution, see: Rappoport, Z.; Biali, S. E. 6th IUPAC Conference on Physical Organic Chemistry, Louvain La Neuve, Belgium, July 11–16, 1982. Abstract: *Bull. Soc. Chim. Belg.* **1982**, *91*, 388.

(2) For a recent review, see: Toullec, J. *Adv. Phys. Org. Chem.* **1982**, *18*, 1.

(3) Bell, R. P. "The Proton in Chemistry", 2nd ed.; Cornell University Press: Ithaca, NY, 1973; p 179.

(4) Dubois, J. E.; El-Alaoui, M.; Toullec, J. *J. Am. Chem. Soc.* **1981**, *103*, 5393. Tapuhi, E.; Jencks, W. P. *Ibid.* **1982**, *104*, 5758.

(5) Hart, H. *Chem. Rev.* **1979**, *79*, 515. Hart, H.; Sasaoka, M. *J. Chem. Educ.* **1980**, *57*, 685.

(6) (a) Capon, B.; Rycroft, D. S.; Watson, T. W. *J. Chem. Soc., Chem. Commun.* **1979**, 724. (b) Capon, B.; Rycroft, D. S.; Watson, T. W.; Zucco, C. *J. Am. Chem. Soc.* **1981**, *103*, 1761. (c) Capon, B.; Siddhanta, A. K. *Tetrahedron Lett.* **1982**, *23*, 3199. (d) Capon, B.; Zucco, C. *J. Am. Chem. Soc.* **1982**, *104*, 7567.

(7) Chiang, Y.; Kresge, A. J.; Walsh, P. A. *J. Am. Chem. Soc.* **1982**, *104*, 6122.

(8) Saito, S. *Chem. Phys. Lett.* **1976**, *42*, 339.

(9) For representative examples of a long series of papers, see: (a) Fuson, R. C.; Armstrong, L. J.; Kneisley, J. W.; Shenk, W. J. *J. Am. Chem. Soc.* **1944**, *66*, 1464. (b) Fuson, R. C.; Armstrong, L. J.; Chadwick, D. H.; Kneisley, J. W.; Rowland, S. P.; Shenk, W. J.; Soper, Q. F. *Ibid.* **1945**, *67*, 386. (c) Fuson, R. C.; Chadwick, D. H.; Ward, M. L. *Ibid.* **1946**, *68*, 389. (d) Fuson, R. C.; Maynert, E. W.; Tan, T. L.; Trumbull, E. R.; Wassmundt, F. W. *Ibid.* **1957**, *79*, 1938 and references therein.

(10) E.g., a review: Forsén, S.; Nillson, M. In "The Chemistry of the Carbonyl Group"; Zabicky, J., Ed.; Interscience: London, 1970; Vol. 2, Chapter 3. An advanced textbook: March, J. "Advanced Organic Chemistry", McGraw-Hill: New York, 1977; p 72.

(11) (a) Bailey, P. S.; Ward, J. W.; Potts, F. E.; Chang, Y. G.; Hornish, R. E. *J. Am. Chem. Soc.* **1974**, *96*, 7228. (b) Miller, A. R. *J. Org. Chem.* **1976**, *41*, 3599.

(12) (a) Biali, S. E.; Lifshitz, C.; Rappoport, Z.; Karni, M.; Mandelbaum, A. *J. Am. Chem. Soc.* **1981**, *103*, 2896. (b) Biali, S. E.; Depke, G.; Rappoport, Z.; Schwarz, H. *Ibid.*, following paper in this issue.

0002-7863/84/1506-0477$01.50/0

for an unusual reaction of their cation radicals in the gas phase[12b] should be also reflected in their static and dynamic NMR behavior, and we therefore studied these features with several enol–ketone pairs.[1b]

The present paper deals mainly with Fuson's most crowded enol, i.e., trimesitylvinyl alcohol (**1**), an enol that could not be ketonized

$$(Mes)_2C{=}C(OH)Mes \qquad Mes = 2,4,6\text{-}Me_3C_6H_2$$
1

under usual conditions.[9] An X-ray diffraction study showed that **1** in the solid state is a distorted molecular propeller where the aryl groups (i.e., the propeller "blades" radiating from the double bond) are all twisted in the same sense.[13] The NMR (see below) revealed that the most likely conformation in solution is also a propeller. Hence, **1** is a member of the family of "vinyl propellers", and indeed the available X-ray data for 1,1-diarylethylenes,[14a] triarylethylenes,[14b] and tetraarylethylenes[14c] show that all of them have a propeller conformation in the solid state. The static and dynamic behavior of these propellers was not investigated very much, and we are unaware of a hitherto stereochemical study of the NMR and DNMR behavior of triarylvinyl propellers. Since the stereochemical behavior is an important property of our enols, we first analyze the static and dynamic stereochemistry of vinyl propellers, and then we describe the specific behavior of **1** and its derivatives.

Static Stereochemistry of Vinyl Propellers. Vinyl propellers of the general formula $Ar^3Ar^2Z{=}W(X)Ar^1$ (Z = C, Si; W = C, Si, N, O^+, S^+), which are exemplified below by the special case when Z = W is C=C (**2**), are analogues of the molecular pro-

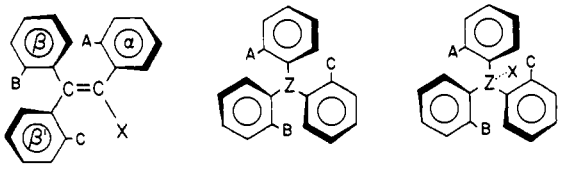

2 **3** **4**

pellers $Ar^1Ar^2Ar^3Z$ (**3**) and $Ar^1Ar^2Ar^3ZX$ (**4**) (Z = C, B, N), which were studied thoroughly by Mislow and co-workers.[15-19] In both formulas A, B, and C are substituents, and X are ligands with local conical symmetry such as H, Me, halogen or pseudoligands such as an electron pair.

Three structural features give rise to isomerism in molecules **4**: (i) chirality center when the four ligands attached to Z are different; (ii) chirality plane since a substituent can be "up" or "down" with regard to the reference plane defined by the three ipso carbons of the aryl groups attached to Z; (iii) chirality axis (helicity). In molecules **3** the first feature is absent. Mislow[16a] termed the structures having three different aryl rings, none of which possesses a local C_2 axis (i.e., A, B, or C are not para substituents), as "maximum labeled". For maximum-labeled systems **3** and **4**, there are 16 and 32 isomers possible, respectively. They are derived from the four enantiomeric pairs arising by

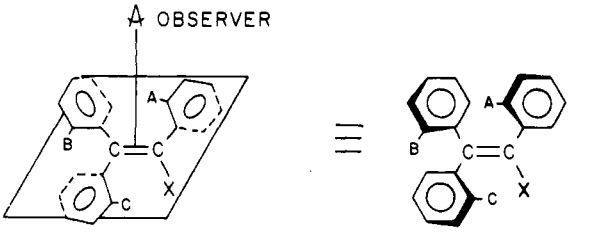

Figure 1. Top view of a vinyl propeller (left) with its corresponding projection (right).

Table I. Isomer Numbers For Systems **2**–**5**

no. of identical rings	system			
	2[a]	**3**[b]	**4**[b]	**5**[a]
	Zero Rings with Local C_2 Axes			
0	96 (16)	16	32	48 (16)
2	48 (16)	8	16	24 (16,[c] 8[d])
3	16 (16)	4	8	8 (8)
	One Ring with Local C_2 Axis			
0	48 (8)	8	16	24 (8)
2	24 (8)	6	8	14 (8,[c] 6[d])
3	0 (0)	0	0	0 (0)
	Two Rings with Local C_2 Axes			
0	24 (4)	4	8	12 (4)
2	12 (4)	2	4	6 (4[c])
3	0 (0)	0	0	0 (0)
	Three Rings with Local C_2 Axes			
0	12 (2)	2	4	6 (2)
2	6 (2)	2	2	4 (2[c,d])
3	2 (2)	2	2	2 (2)

[a] Including positional and configurational isomers. The number of stereoisomers for a single configuration is given in parentheses. [b] From ref 15. [c] When $Ar^1 = Ar^2$. [d] When $Ar^2 = Ar^3$.

permutations of "up" and "down" substituents, each of which can be of a different helicity and with an *R* or an *S* configuration.

In the vinyl propellers **2**[20] only the plane of chirality and the helicity can be present. The highest symmetry possible is C_1, in contrast to the D_3 and C_3 symmetries for **3** and **4**, respectively. Consequently, there are only eight enantiomeric pairs of structure **2**, i.e., for a given configuration the maximum number of labeled propellers is 16. We follow Mislow[16] in describing each isomer unequivocally by a set of four digits in brackets, where each digit is either zero or one. Arbitrarily,[21] the first digit describes the helicity, and 1 and 0 designate right- and left-handed propellers, respectively. The second, third, and fourth digits relate to the position of the substituent in the α, β, and β' rings in this order, where α is the ring on the X-substituted carbon C_α, β is the ring cis to it, and β' is the ring trans to it on C_β. For drawing the three-dimensional propeller in a two-dimensional projection we view the molecule from the plane of the π(C=C) bond along an axis that dissects this bond, in a way that the substituent X is always oriented to the bottom right. The edge pointing to the observer is thickened (Figure 1) and a substituent (A, B, or C) on it that is above ("up") the molecular plane defined by C_α, C_β, and the atom of X attached to C_α is assigned the digit 1. When it is below ("down") this plane, it is assigned the digit 0. For demonstration, the eight isomers of the right-handed helicity with their corresponding labels are drawn in Figure 2.

(13) Kaftory, M.; Biali, S. E.; Rappoport, Z., manuscript in preparation.
(14) E.g.: (a) Casalone, G.; Mariani, C.; Mugnoli, A.; Simonetta, M. *Acta Crystallogr.* **1967**, *22*, 228. Casaloni, G.; Gavezzotti, A.; Mariani, C.; Mugnoli, A.; Simonetta, M. *Acta Crystallogr., Sect. B* **1970**, *B26*, 1. Casalone, G.; Simonetta, M. *J. Chem. Soc. B* **1971**, 1180. (b) Tucker, P. A.; Hoekstra, A.; Ten Cate, J. M.; Vos, A. *Acta Crystallogr., Sect. B* **1975**, *B31*, 733. Kaftory, M.; Apeloig, Y.; Rappoport, Z., unpublished results. (c) Hoekstra, A.; Vos, A. *Acta Crystallogr., Sect. B* **1975**, *B31*, 1716. Blount, J. F.; Mislow, K.; Jacobus, J. *Acta Crystallogr., Sect. A* **1972**, *A28*, S12.
(15) Gust, D.; Mislow, K. *J. Am. Chem. Soc.* **1973**, *95*, 1535.
(16) (a) Mislow, K. *Acc. Chem. Res.* **1976**, *9*, 26. (b) Mislow, K.; Gust, D.; Finocchiaro, P.; Boettcher, R. J. "Topics in Current Chemistry No. 47, Stereochemistry 1"; Springer-Verlag: Berlin, 1974; p 1.
(17) (a) Finocchiaro, P.; Gust, D.; Mislow, K. *J. Am. Chem. Soc.* **1973**, *95*, 7029; (b) *Ibid.* **1974**, *96*, 2165; (c) *Ibid.* **1974**, *96*, 2176. (d) Andose, J. D.; Mislow, K. *Ibid.* **1974**, *96*, 2168. (e) Kates, M. R.; Andose, J. D.; Finocchiaro, P.; Gust, D.; Mislow, K. *Ibid.* **1975**, *97*, 1772.
(18) Hummel, J. P.; Gust, D.; Mislow, K. *J. Am. Chem. Soc.* **1974**, *96*, 3679.
(19) (a) Hayes, K. S.; Nagumo, M.; Blount, J. F.; Mislow, K. *J. Am. Chem. Soc.* **1980**, *102*, 2773. (b) Glaser, R.; Blount, J. F.; Mislow, K. *Ibid.* **1980**, *102*, 2777.
(20) The vinyl propellers **2** are derived from the triaryl propellers **4**, Z = C, by insertion of a C= unit between the Ar^3Ar^2C and the Ar^1 and X moieties. In this respect they can be formally termed the "carbonologues" of **4**.
(21) Other notations, e.g., the use of U and D for "up" and "down" and "+" and "–" for the chirality, which are more self-explanatory, are possible. However, we prefer the present notation, which emphasizes the analogy with the notation used for **3** and **4**.
(22) Stang, P. J.; Rappoport, Z.; Hanack, M.; Subramanian, L. R. "Vinyl Cations"; Academic Press: San Francisco, 1979.

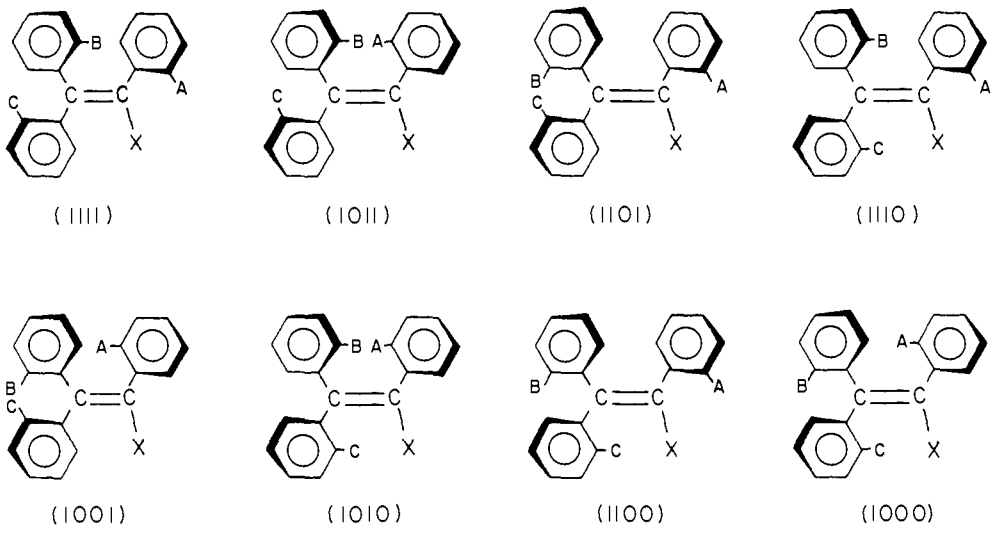

Figure 2. Eight isomers of a vinyl propeller of one helicity with their corresponding designations.

The presence of the double bond in **2** distinguishes it from **3** and **4** and introduces configurational and positional isomerism. Consequently, the maximum number of isomers increases and becomes 96 when all the rings are different and lack a local C_2 axis. The numbers of isomers of systems **2**–**4** and of the vinyl carbocation **5** are compared in Table I. In the first and the second

$$\underset{\mathbf{5}}{Ar^2(Ar^3)C{=}\overset{+}{C}Ar^1}$$

rows, the number of isomers of **2** is 3 times larger than that of **4**, while in the third row it is 2 times larger or equal. When $Ar^1 \neq Ar^2 \neq Ar^3$ (first row), this is due to the six permutations of the rings around the C=C bond and the lack of chirality center in **2**. When $Ar^1 \neq Ar^2 = Ar^3$ (second row), an independent chirality center in **4** is absent, and the factor of 3 arises from the three permutations of the aryl rings in **2**. When $Ar^1 = Ar^2 = Ar^3$ (third row) and C_2 axes are absent, four permutations of the substituents with regard to the chirality plane are possible in system **4** of a given helicity, in contrast with **2** where eight permutations are possible.

Heterolytic cleavage of the C-X bond of **2** generates the linear vinyl cation **5** in which the α-ring is perpendicular to the double-bond plane. The same chirality elements are common to **2** and **5**, and therefore for the maximum-labeled systems (first row) both systems have the same number of isomers. When positional and configurational isomers are counted, the number of isomers of **2** is twice as large, since there are no *E*,*Z* isomers in **5**.

When two rings are identical, only two permutations in **5** and three permutations in **2** are possible. Moreover, due to the presence of a molecular C_2 axis in some isomers of **5**, less permutations of the substituents with regards to the chirality plane are possible. The number of isomers of **5** is always equal to or larger than that for the sp^2 hybridized ion **3** (Z = C^+). This is due to the possible existence of positionally isomeric ions **5** where at least two rings are different and to the presence of a chirality plane.

An additional feature (not included in Table I) that may increase the number of isomers of **2** appears when the group X lacks a conical symmetry.[23] For example, when X = OY rotation around the C–O bond leads to several distinct conformers which differ in the mutual positions of the double bond and Y. These may be syn and gauche as calculated for methyl vinyl ether[24] or syn and anti as found for simple aliphatic enols.[5c]

Only a few stereoisomers **3** and **4** have been separated,[19b] and only one pair of helicity isomers (of **3**) was resolved.[19a] Although *E*,*Z* mixtures or positional isomers of **2** are frequently separated,[25] vinyl propellers of one configuration were not separated or resolved so far.

Dynamic Stereochemistry of Vinyl Propellers. Several processes may interconvert some or all of the 96 isomers of a maximum-labeled vinyl propeller. Although only several of them are observed in the present study, which involves systems with much higher symmetry than the maximum-labeled ones, some of the other processes may take place in closely related systems.[26] We therefore present here a brief general analysis of the possible stereoisomerization routes, which will serve as a reference to our future work on related systems. Further detailed analysis of the specific systems studied here is given under Discussion. We consider the following stereoisomerization routes according to the increased "apparent" difficulty of the process involved, by using the C=C bond as a representative of the general Z=W bond.

(i) Rotation around the C(sp^2)–C(Ar) Bonds. Such rotations in molecular propellers are correlated in the sense that the rotation of the three rings is coupled and takes place simultaneously in a geared motion. They are commonly discussed in terms of "flip" mechanisms, first suggested by Kurland[27] and extended by Mislow,[15-19] each of which involves helicity reversal. A flip is a passage through a plane perpendicular to the reference plane with no edge interchange, while the nonflipping rings rotate concomitantly in the opposite direction and pass through the reference plane with edge interchange. Depending on the number of flipping rings during the rotation the mechanisms are designated as zero-, one-, two-, or three-ring flips. The various transition states for the propellers **4** were given by Mislow.[16b] An analogous set of transition states for the flip mechanisms of **2** could be given but with an important difference. Identity of the rings of **3** or **4** introduces degeneracy into the 1- and 2-ring flip routes, but due to the different geometrical relationships between chemically identical rings in **2**, the three one-ring flips which involve the α, β, or β' ring are nondegenerate. The same is true for the three two-ring flips. In Figure 3 we arbitrarily show one set of flip routes where the one-ring flip involves the α-ring and the two-ring flip involves the flipping α and β rings.

Table II shows the interconversions of pairs of isomers of **2** by a single-flip mechanism. Alternatives to the single-step mechanisms are consecutive flip mechanisms which can lead from any stereoisomer in the table to another and which can also be deduced by inspecting the table. The flipping ring or rings are given in square brackets and the zero-ring flip mechanism is indicated by "[0]". It can readily be seen from Table II that the only single-flip mechanism resulting in enantiomerization, e.g., (1111) ⇌ (0000),

(23) Table I can be used when the rotation of the OY group is rapid on the time scale of the experiment. Under these conditions the substituent behaves as if it has a conical symmetry.

(24) Dudziuk, H.; von Voithenberg, H.; Allinger, N. L. *Tetrahedron* **1982**, *38*, 2811.

(25) E.g.: Rappoport, Z.; Apeloig, Y. *J. Am. Chem. Soc.* **1969**, *91*, 6734. Rappoport, Z.; Houminer, Y. *J. Chem. Soc., Perkin Trans. 2* **1973**, 1506.

(26) Biali, S. E.; Rappoport, Z., unpublished results.

(27) Kurland, R. J.; Schuster, I. I.; Colter, A. K. *J. Am. Chem. Soc.* **1965**, *87*, 2279.

Table II. Interconversion of Stereoisomers in Systems 2 by the Flip Mechanisms

stereoisomer	(0111)	(0110)	(0101)	(0011)	(0100)	(0010)	(0001)	(0000)
(1111)	[α,β,β']	[α,β]	[α,β']	[β,β']	[α]	[β]	[β']	[0]
(1110)	[α,β]	[α,β,β']	[α]	[β]	[α,β']	[β,β']	[0]	[β']
(1101)	[α,β']	[α]	[α,β,β']	[β']	[α,β]	[0]	[β,β']	[β]
(1011)	[β,β']	[β]	[β']	[α,β,β']	[0]	[α,β]	[α,β']	[α]
(1100)	[α]	[α,β']	[α,β]	[0]	[α,β,β']	[β']	[β]	[β,β']
(1010)	[β]	[β,β']	[0]	[α,β]	[β']	[α,β,β']	[α]	[α,β']
(1001)	[β']	[0]	[β,β']	[α,β']	[β]	[α]	[α,β,β']	[α,β]
(1000)	[0]	[β']	[β]	[α]	[β,β']	[α,β']	[α,β]	[α,β,β']

Table III. Interconversions of the Stereoisomers of $(o\text{-}AC_6H_4)_2C{=}C(X)C_6H_4A\text{-}o$ by Nonflip Routes[a]

isomer	(1111)	(1110)	(1101)	(1011)	(1100)	(1010)	(1001)	(1000)
(1111)	I, R				D			I, R, L
(1110)		D, I	R	R	R	I, L	R	
(1101)		R	D, I	R	R	R	I, L	
(1011)		R	R	I	I, L	R	R	D
(1100)	D	R	R	I, L	I	R	R	
(1010)		I, L	R	R	R	D, I	R	
(1001)		R	I, L	R	R	R	D, I	
(1000)	I, R, L			D				I, R

[a] The table applies similarly to the interconversion of the isomers of $(o\text{-}CC_6H_4)C(o\text{-}BC_6H_4){=}C(X)C_6H_4A\text{-}o$ of molecule 2. Processes given: D, double-bond rotation or electrophilic addition-rotation-elimination process. I, ionization-recombination. R, ionization-β-aryl rearrangement-recombination. L, inversion (lateral shift mechanism).

is the zero-ring flip. Other flip mechanisms lead to diastereoisomerization, e.g., starting from the isomer (0011) an [α] ring flip gives the diastereomer (1000), a two-ring [α,β] flip, followed by a one-ring [β'] flip will give the diastereomer (0100) and a three-ring [α,β,β'] flip leads to the diastereomer (1011). Three consecutive one-ring flips in any order (i.e., [β'], [α], [β]) or a three-ring [α,β,β'] flip will give the same diastereomer, e.g., to (1110) from (0110). On the other hand, three consecutive two-ring flips in any order (i.e., [α,β], [α,β'], [β,β']) lead to enantiomerization, e.g., to (1001) from (0110).

Table II can be also used when one or more of the rings have a local C_2 axis. In this case the digit describing this ring is irrelevant and the designations are modified by replacing the digit with a dash. An example for the combined use of Tables I and II is the previously studied enol **6**,[1b] where only the α ring lacks

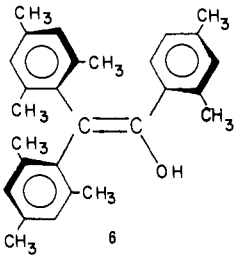

6

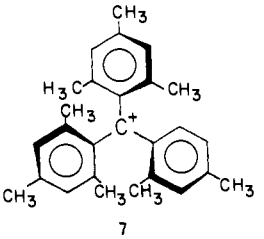

7

a C_2 axis. The questions to answer are how many isomers of **6** exist and which flip mechanism can lead to enantiomerization? Table I indicates that only four isomers can exist and these are (11--), (10--), (01--), and (00--), while Table II shows that the two enantiomerization processes of interest, i.e., (11--) ⇌ (00--) and (10--) ⇌ (01--), can proceed via four different single-step mechanisms, i.e., [β,β']-, [β]-, [β']-, or [0]-ring flips.

In contrast, there are only two "helicity" enantiomers of the analogue **7** since no chirality plane is present. They can interconvert by any of the possible eight ([α,β,β'], [α,β], [α,β'], [β,β'], [α], [β], [β'], and [0]) single-flip mechanisms since each one of them involves helicity reversal.

In discussing the following stereoisomerization routes (double-bond rotation, addition–elimination, ionization followed by rearrangement or recombination), each one is treated as an independent process. For example, ionization to **5**, followed by a flip process, may take place and may even dominate the overall process. However, in our analysis we will discuss only the important stereochemical features that result from the ionization process itself, without including the consequences of intervention by superimposable routes. The assumptions involved in our

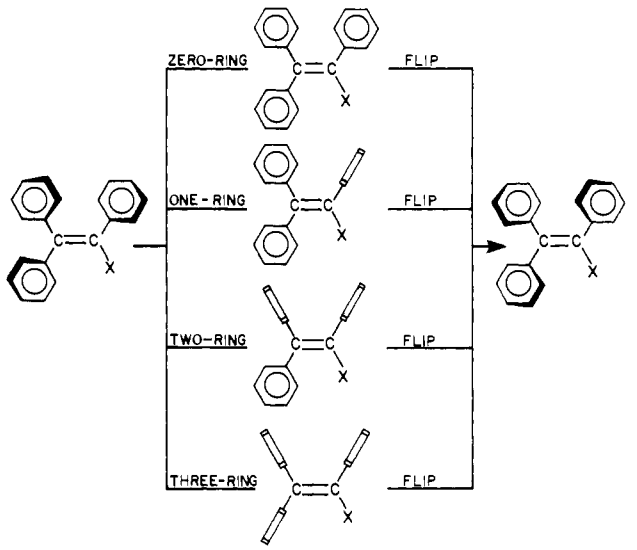

Figure 3. Examples of the various transition states for the flip mechanisms for a vinyl propeller ▭ indicates a ring that is perpendicular to the C=C plane.

treatment are that whenever possible the molecule will prefer to retain its propeller conformation and that the rings will always prefer to undergo the least torsional motion.

(ii) Rotation around the Double Bond. A rotation around the double bond (eq 1) is energetically expensive in simple systems.

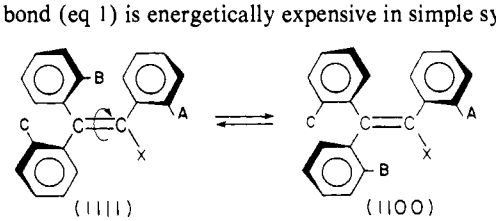

(1)

However, the rotational barriers are reduced and rotation takes place when the substituents are highly twisted from the plane of the double bond[28] or when the ethylenes are of the push–pull type.[28] Such rotation will lead to interchange of the rings β and β' and to edge interchange. The helicity is retained throughout the rotation and the process therefore leads to geometrical but not to positional isomerization and to diastereomerization but not to

(28) Kalinowski, H. O.; Kessler, H. *Top. Stereochem.* **1973**, *7*, 295.

Scheme I

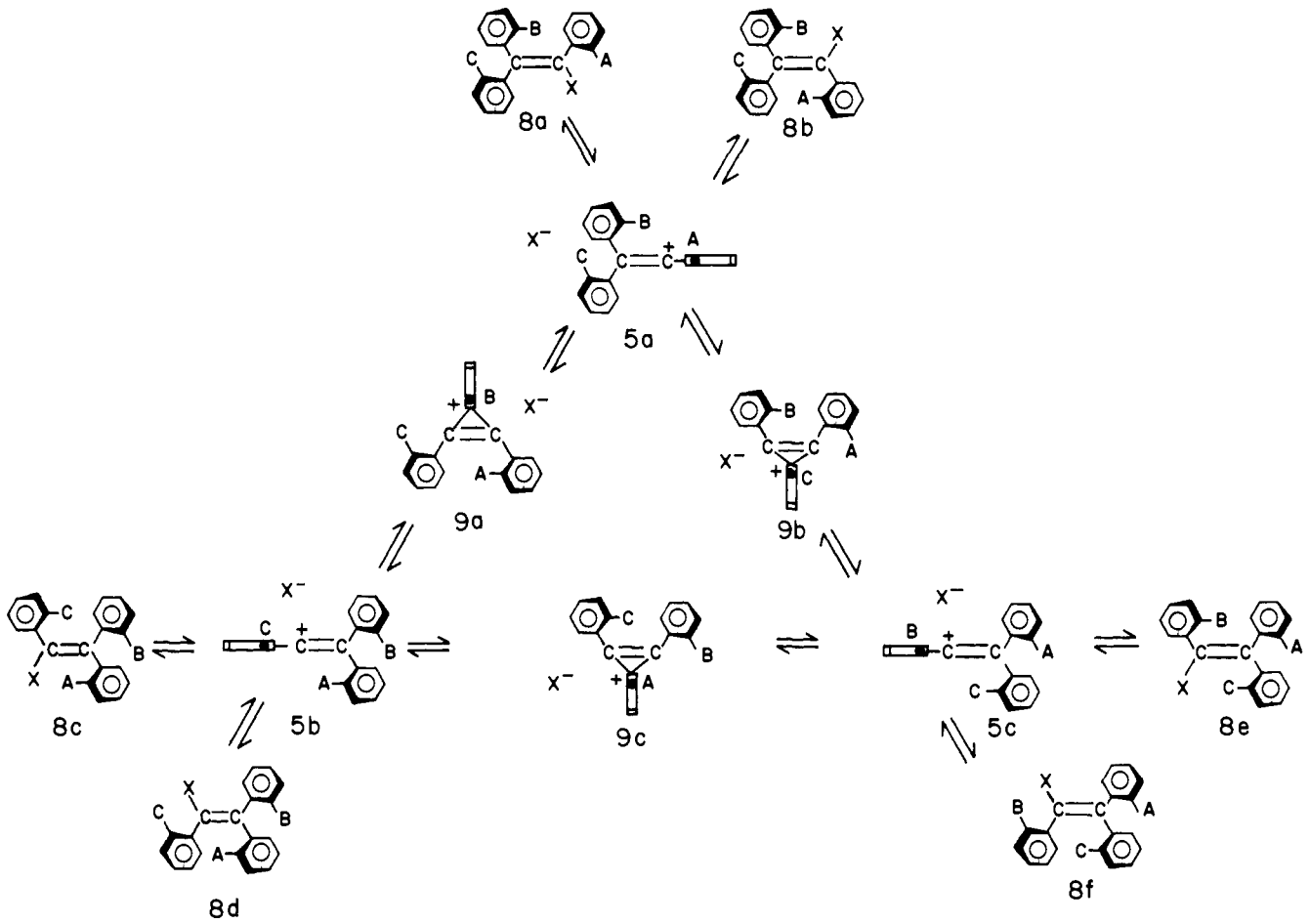

enantiomerization. The isomers obtained by this route are shown in Table III under the designation D.

(iii) Geometrical and Positional Isomerizations. Both geometrical and positional isomerizations can be achieved via a reversible heterolysis of **2** to the vinyl cation **5** (Scheme I). Vinyl cations have relatively low stability compared with the tetrasubstituted precursors.[22] Hence, for the reaction to occur, X should be a very good nucleofuge or the activation for the ionization by the α-aryl group should be high. The ionization **8a** → **5a** is accompanied by angle changes involving all the aryl rings. The sp^2 → sp hybridization change which accompanies the ionization changes the α-Ar–C=C angle from 120° to 180°. Maximum stabilization of **5a** is achieved when the $\pi(\alpha\text{-Ar})$ and the $p(C^+)$ orbitals are parallel, resulting in a change of the dihedral angle between the C=C and the α-aryl planes from a value between 0° and 90° in **8a** to 90° in **5a**. Loss of X and linearization at C_α also relieve the steric interactions in **8a** between the β rings and the α-substituents with a consequent opening of the β-Ar–C_β–β'-Ar angle and reduction of the torsional angles of the two rings in order to increase the $\pi(C{=}C)$–$\pi(\beta$ and β'-Ar) overlap. The angle change is apparently not large since the torsional angle in 1,1-diarylethylenes is still appreciable,[13a] and the energy gained by the somewhat larger $\pi(\beta\text{-Ar})$–$\pi(C{=}C)$ overlap is small. More important, the low-energy path retains the helicity, and the overall ionization process converts **8a** with the C_1 symmetry to **5a** of a maximum symmetry C_2 with the same helicity.

Ion **5a** can undergo several processes. First, recombination with the nucleofuge X from either of its diastereotopic faces will give the starting material **8a** in a stereochemically hidden retention process or its geometrical isomer **8b** in an inversion process (Scheme I). The helicity of the ion is determined by the β-aryl groups, and if the recombination occurs before any flip in **5a** takes place, there will be no helicity reversal. This situation is analogous to substitution in the molecular propellers **4**, where inversion does not lead to helicity reversal.[15] As in case ii above, this route can lead to the geometrical isomers when β-Ar ≠ β'-Ar, but not to enantiomerization, as shown in Table III. Related ionization–recombination routes in saturated systems were detected by DNMR.[29]

Second, interconversion of positional isomers is achieved by permutation of the aryl groups between C_α and C_β and requires the cleavage of at least two bonds. This can take place via a β-aryl rearrangement across the double bond of **5a** when one of the rings on C_β is better electron donator than the α-aryl ring, followed by recombination with X. Scheme I demonstrates the two possible migrations of the β and the β' ring via the bridged transition states **9a** and **9b**,[31] respectively. When the three rings are identical (i.e., A = B = C) several consecutive degenerate β-aryl rearrangements can take place before the recombination with X. This is demonstrated in Scheme I by the **5a** → **9a** → **5b** → **9c** → **5c** → **9b** process. There are precedents for both degenerate and nondegenerate rearrangements.[22,30]

The ionization–rearrangement–recombination process involves changes in the positions and torsional angles of all the rings. Starting with the **5a** → **9a** process as an example, the bridging carbon of the β-ring undergoes tetrahedralization on bridging, and the migrating β ring moves in the plane of C_α, C_β, and its ipso carbon and concomitantly rotates in a counterclockwise motion to a perpendicular plane. The other two rings also move and rotate. The β ring moves away and the α ring moves closer

(29) (a) Kessler, H.; Feigel, M. *Acc. Chem. Res.* **1982**, *15*, 2. (b) Ōki, M.; Shimizu, A.; Kihara, H.; Nakamura, N. *Chem. Lett.* **1980**, 607.

(30) E.g.: Rappoport, Z.; Noy, E.; Houminer, Y. *J. Am. Chem. Soc.* **1976**, *98*, 2238. Houminer, Y.; Noy, E.; Rappoport, Z. *Ibid.* **1976**, *98*, 5632. Lee, C. C.; Obefami, C. A.; Rappoport, Z. *Can. J. Chem.* **1982**, *60*, 3019 and references therein. Reference 22, chapter 7.

(31) Although there is evidence that in the β-aryl rearrangements in triarylvinyl cations studied so far the bridged species is a transition state and not an intermediate,[30] for convenience we treat it in Scheme I and in the discussion as a stable discrete ion.

to the β' ring, and charge is partly created on C_β. A π(Ar)–p(C^+) interaction is probably more stabilizing than a π(Ar)–π(C=C) interaction, and if A, B, and C are good electron-donating groups and an appreciable charge resides on both C_α and C_β, in the limiting case both the α and the β rings will prefer to achieve a conformation (not shown in Scheme I) when they are perpendicular to the plane of the double bond. The structure of **9a** with the three perpendicular aryl rings to the C=C plane is reminiscent of the transition state of the three-ring flip, with the difference that one aryl group bridges C_α and C_β.

A different structure of **9a** is possible when A, B, and C are strongly electron-withdrawing substituents. The π(Ar)–π(C=C) interaction may then be more stabilizing than the π(Ar)–$p(C^+)$ interaction. The β'- and α-aryl group will then rotate in a clockwise direction, but **9a** will still retain its chirality and helicity.

The rearrangement is completed by movement of the β ring to C_α and linearization at C_β. When the three rings are perpendicular, there is no limitation on the helicity that the α and the β rings can achieve, and the rearranged open ion **5b** will be obtained in two helicities. In the latter case, when the rings are not perpendicular the helicity will be retained throughout the process. Recombination of **5b** with X^- at C_β will give the positional and geometrical isomers **8c** and **8d** with helicities as discussed above. If the rearrangement is degenerate, recombination can take place at both C_α and C_β. It should be noted that in Scheme I none of the rings pass via the C=C plane, so that the mutual relationship between "up" and "down" substituents is retained throughout the process. Several interconversions of stereoisomers are given in Table III.

Both the open (**5a–c**) and the bridged (**9a–c**) species[31] can undergo internal rotations which differ in two respects from the analogous processes in the neutral precursor. First, the α ring in the open ion and all the three rings in the totally perpendicular bridged species are "frozen" due to the overlap with the p(C^+) orbital, and their rotations will be energetically more costly. Second, the steric interaction between the three aryl groups is larger in the covalent sp^2-hybridized **2** than in the linear cation **5** in spite of the shorter bonds in the latter. This will facilitate the rotation of the β rings in **5**.

An analogous case is a vinyl propeller where one of the atoms of the double bond carries an electron pair. This may be a carbanionic center (W = C^- in **10a**) or an imine (W = N, in **10a**).[32] An inversion mechanism converting **10a** to **10b** (the "lateral shift mechanism")[33] could then take place (eq 2) with

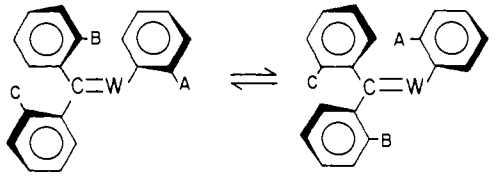

(2)

10a 10b

interchange of the positions of rings β and β', and without concomitant edge interchange or helicity reversal.

(iv) Electrophilic Addition–Rotation–Elimination Route. A mechanism that is unique to vinylic systems is an electrophilic addition–rotation–elimination route (Scheme II), which has precedents.[34] Addition of a proton from the acidic solvent (e.g., AcOH) generates either the 1,2,2-triarylethyl cation **11** (addition to C_β) or the 1,1,2-triarylethyl cation **12** (addition to C_α). In both cases stabilization will be achieved when one or more of the aryl groups will be in the plane originally belonging to the double bond.[35] In addition, rotation around the C_α–C_β bond in these

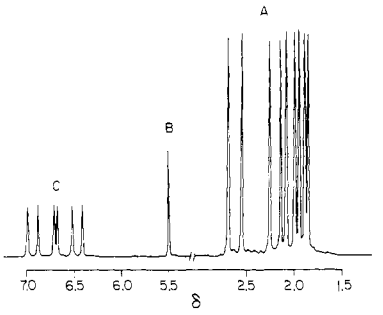

Figure 4. ^{1}H 300-MHz NMR spectrum of **1** in $C_6D_5NO_2$ at room temperature. A: Me groups region; B: OH group; C: aromatic region.

Scheme II

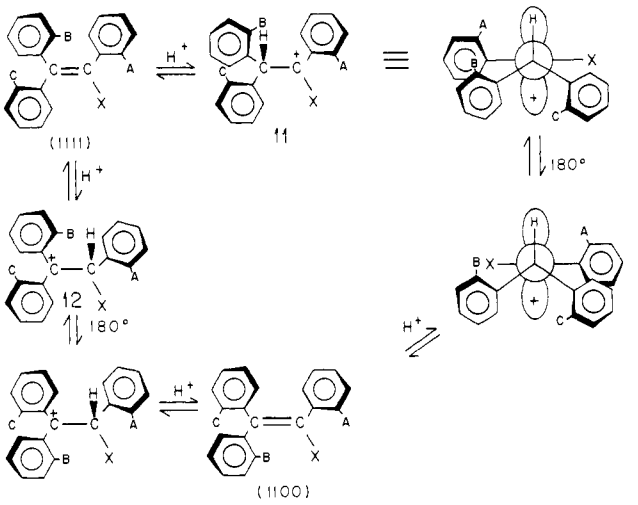

ions can take place, resulting in stereoisomerization after the proton expulsion, as shown in Table III. It should be noted that the two faces of the double bond are diastereotopic, and the protonation should therefore occur preferentially from one of the faces.

(v) Ketonization–Reenolization Route. A ketonization–reenolization route (eq 3) is unique for enol systems (i.e., **2**, X = OH).

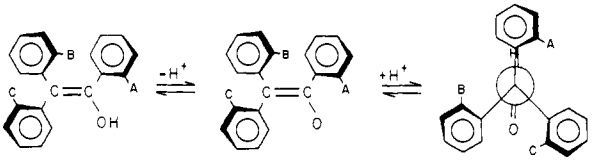

(3)

An acid- or base-catalyzed stepwise enolization can take place in an acidic or a basic solvent. In the example given, neither the ionization of the enol nor the reprotonation are expected to change the helicity. A propeller conformation of the ketone is assumed as found for a sterically hindered triarylethanone.[13] The ketone itself may undergo rotation around the CH–CO, CH–Ar, or CO–Ar bonds before returning to the enol. Without a knowledge of the rotational barriers, we cannot predict the preferred rotations that would lead to stereoisomerization. The reenolization is not expected to change the helicity of the ketone.

Results and Discussion

Trimesitylethenol: Static NMR and Assignment. Trimesitylethenol (**1**) was synthesized from dimesityl ketene and mesitylmagnesium bromide by a slight modification of Fuson's method[9c] (eq 4). Like Fuson, we were unable to detect the corresponding

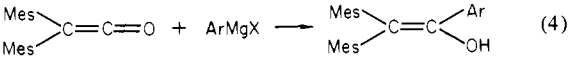

(4)

I, Ar = Mes
13, Ar = 2,4,6-$(CD_3)_3C_6H_2$(Mes*)
14, Ar = 2,6-$Me_2C_6H_3$

ketone, trimesitylethanone, in the reaction mixture. Another

(32) Curtin, D. Y.; Grubbs, E. J.; McCarty, C. G. *J. Am. Chem. Soc.* **1966**, *88*, 2775.
(33) Reference 28, p 332.
(34) Peterson, P. E.; Indelicato, J. M. *J. Am. Chem. Soc.* **1968**, *90*, 6515. Rappoport, Z.; Gal, A. *J. Chem. Soc., Perkin Trans. 2* **1973**, 301.
(35) For a discussion of the opposite stereochemical requirement of an α-aryl group in vinylic solvolysis and in electrophilic addition–elimination, see: Rappoport, Z.; Shulman, P.; Thuval (Shoolman), M. *J. Am. Chem. Soc.* **1978**, *100*, 7041.

Table IV. Assignment and Solvent Effects on the Chemical Shifts of the Protons of 1[a]

	solvent									
assignment	$C_6D_5CD_3$	C_6D_6	C_6D_5Br	CCl_4	C_6D_{12}	$CDCl_3$	$C_6D_5NO_2$	CD_3CN	CD_3COCD_3	CD_3SOCD_3
α-*o*-Me	1.99	2.03 or 2.04	1.94	1.82	1.85	1.88	1.93	1.88	1.90	1.83
α-*p*-Me	2.04	2.03 or 2.04	2.07	2.20	2.15	2.21	2.14	2.19	2.18	2.17
α-*o*-Me	2.48	2.51	2.46	2.38	2.39	2.43	2.54	2.40	2.46	2.37
$\Delta\nu$(α-*o*-Me)[b]	0.49	0.48 or 0.47	0.52	0.54	0.54	0.55	0.61	0.52	0.56	0.54
OH	4.90	4.94	5.08	5.10	5.11	5.20	5.46	5.84	6.83	8.34
α-Mes H	6.44	6.47	6.41	6.53	6.51	6.61	6.39	6.60	6.57	6.59
α-Mes H	6.88	6.83	6.82	6.94	6.77	6.88	6.87	6.91	6.89	6.89
$\Delta\nu$(α-Mes H)[b]	0.44	0.36	0.41	0.41	0.26	0.27	0.48	0.31	0.32	0.30
β′-*o*-Me	1.92	1.96	1.89	1.80	1.81	1.85	1.84	1.79	1.81	1.70
β′-*o*-Me	2.61	2.62	2.62	2.58	2.58	2.61	2.68	2.55	2.61	2.50[b]
$\Delta\nu$(β′-*o*-Me)[b]	0.69	0.66	0.73	0.78	0.77	0.76	0.84	0.76	0.80	0.80
β-*o*-Me	1.94	1.98	1.90	1.77	1.80	1.83	1.87	1.79	1.82	1.74
β-*o*-Me	2.01	2.06	1.97	1.79	1.83	1.86	1.98	1.86	1.90	1.80
$\Delta\nu$(β-*o*-Me)[b]	0.07	0.08	0.07	0.02	0.03	0.03	0.11	0.07	0.08	0.06
β-*p*-Me	1.99	2.00	2.01	2.12	2.08	2.14	2.08	2.11	2.10	2.08
β′-*p*-Me	2.16	2.15	2.22	2.25	2.22	2.27	2.25	2.24	2.23	2.20
$\Delta\nu$[(β′-*p*-Me)-(β-*p*-Me)]	0.17	0.15	0.21	0.13	0.14	0.13	0.17	0.13	0.13	0.12
β-Mes H	6.54	6.59	6.51	6.51	6.51	6.59	6.50	6.59	6.57	6.53
β-Mes H	6.60	6.64	6.61	6.54	6.77	6.63	6.67	6.65	6.64	6.59
$\Delta\nu$(β-Mes H)[b]	0.06	0.05	0.10	0.03	0.26	0.04	0.17	0.06	0.07	0.06
β′-Mes H	6.68	6.70	6.71	6.73	6.74	6.80	6.70	6.76	6.72	6.64
β′-Mes H	6.98	6.89	6.94[c]	6.94	6.95	7.02	6.98	7.00	6.96	6.89
$\Delta\nu$(β′-Mes H)[b]	0.30	0.19	0.23	0.21	0.21	0.22	0.28	0.24	0.24	0.25

[a] All values in δ units downfield from internal Me_4Si at 295 K. [b] Difference in δ values of diastereotopic signals in the same ring. [c] Assumed value since the peak is obscured by a signal for the residual protons of the solvent.

compound, yet unidentified, was also formed in this reaction.

The 300-MHz ^1H NMR spectrum of **1** in $C_6D_5NO_2$ at room temperature showed a separate signal for each proton or a methyl group. Altogether there are 16 separate signals: nine for the methyl groups, six for the aromatic protons, and one for the OH group (Figure 4 and Table IV). Consequently, the spectrum indicates that rotations around all the C(aryl)–C(sp)[2] bonds are restricted. It is consistent with the propeller conformation that was found in the solid state,[13] according to which all methyl groups or aromatic protons are either diastereotopic or constitutionally heterotopic.

Two features in the spectrum are noteworthy. First, the signals of the aromatic protons are broadened as a result of long-range couplings with the meta protons and with the two neighboring methyl groups (literature values: $J_{meta} = 2$, $^4J_{HMe} \sim 0.75$ Hz).[36] By strong irradiation of all the methyl groups to saturation, the signals for the aromatic protons are sharpened and converted to the characteristic doublet of meta coupling with $J_{meta} = 1.98$ Hz. Second, the signal for the OH group appears as a sharp singlet. Its chemical shift is strongly solvent dependent (Table IV).[37]

In order to learn more about the conformation of the molecule in solution, as well as for the study of its dynamic stereochemistry, an unequivocal assignment of the NMR signals is required. This was achieved by a combination of methods which includes the synthesis of the appropriate analogues, deuteration of the methyl groups, the saturation transfer technique, and aromatic-solvent-induced shifts.

The α-mesityl-*methyl-d_9* deuterated analogue **13** was prepared by the method of eq 4 by using mesityl-*methyl-d_9*-magnesium bromide. The labeled bromomesitylene (98.4% methyl deuterated by NMR) was prepared by brominating mesitylene-*methyl-d_9*.[38] The ^1H NMR of **13** in $C_6D_5NO_2$ showed six methyl signals, four broadened singlets, and two doublets in the aromatic region. Comparison of the NMR's of **1** and **13** identified the three methyl groups of **1** that were missing in the spectrum of **13** as those due to the α-mesityl group. The other methyl groups belong to the

Scheme III

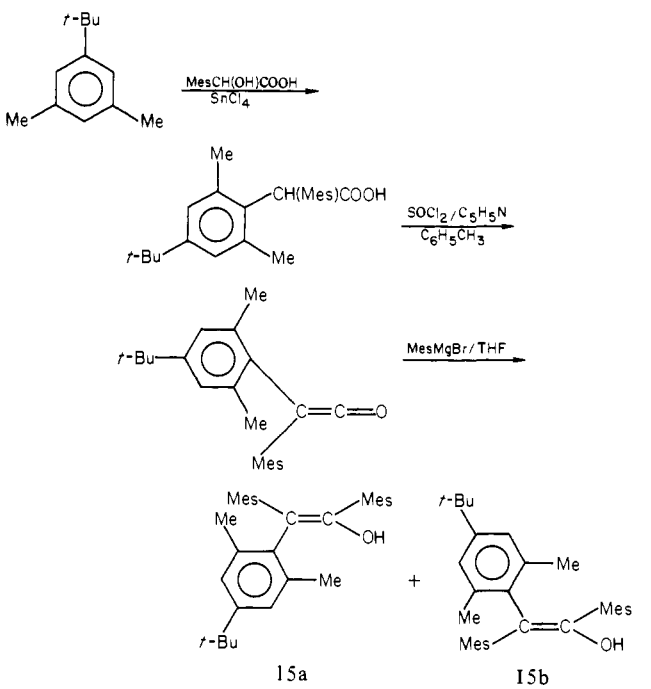

β- and β′-mesityl rings (Table IV). Also, the two aromatic doublets are identified as due to the α-mesityl ring since they showed a meta coupling constant of 1.98 Hz. The coupling with the methyl group is virtually removed by the deuteration since J_{CD_3H} should be 6.5 times smaller than J_{MeH}.[39]

In order to distinguish between the *o*- and *p*-methyl groups of the α-aryl ring, the xylyl analogue **14** was prepared. Its ^1H NMR spectrum showed eight methyl signals, four broad singlets of aromatic protons and one aromatic three-proton multiplet. Comparison of the spectra of **1**, **13**, and **14** identified the Me signal missing in the spectrum of **14** as the *p*-Me signal of the α-mesityl group of **1**. Consequently, the other missing Me groups in the

(36) Günther, H. "NMR Spectroscopy"; Wiley: Chichester, 1980; pp 384–385.

(37) The signal is so sharp that (*E*)- and (*Z*)-**16** show separate OH singlets.[26]

(38) (a) Cheng, T. S.; Mocydlarz, J. W.; Leitch, C. C. *J. Labelled Compd.* **1970**, *6*, 285. (b) Smith, L. I. "Organic Syntheses"; Wiley: New York, 1943, Collect. Vol. II, p 95.

(39) Sandström, J. "Dynamic NMR Spectroscopy"; Academic Press: London, 1982; p 124.

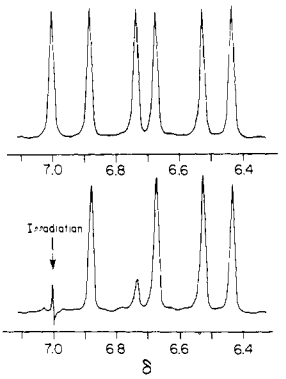

Figure 5. Saturation transfer experiment for identifying pairs of coalescing signals. Top: ^{1}H NMR spectrum of the aromatic region of **1** in $C_6D_5NO_2$ at 321 K before irradiation. Bottom: The same spectrum when the signal at 7.0 ppm is irradiated. Note the intensity diminution of the signal at 6.73 ppm.

spectrum of **13** are due to the *o*-Me group of the α-aryl ring. The aromatic region of **14** resembles that of **13**, except that the two doublets are converted to a multiplet. This reinforces the assignment of the two aromatic protons of the α-aryl ring since the replacement of a *p*-Me group by a proton should lead to the observed upfield shift and to a complex ABC pattern of the protons involved.

Assignment of the *p*-Me groups of the β-aryl rings was assisted by the synthesis of the β-4-*tert*-butyl-2,6-dimethylphenyl analogues **15a,b** from the corresponding ketene and MesMgBr (Scheme III). The NMR of the product showed it to consist of a 60:40 mixture of the *E,Z* isomeric pair **15a,b**. The best probe for distinguishing between the isomers and for determining their ratio is the *tert*-butyl signals, which appear as sharp singlets separated by 61.0 Hz in the 300-MHz ^{1}H NMR spectrum in $C_6D_5NO_2$. It is interesting that the sharp OH signals of the two isomers are also separated from one another by 24.2 Hz. Comparison of the spectrum with that of **1** enables the identification of the two *p*-Me groups on the β and the β′ rings in the spectrum of **1**. Fractional crystallization of the **15a–15b** mixture enriched the mixture to >90% of one isomer, probably **15a**, and enabled identification of the two aromatic protons associated with the *tert*-butyl-carrying ring. In addition to evidence from integration, the two aromatic protons in this ring appear as a doublet with J_{meta} = 1.98 Hz, which is broadened by coupling with the methyl groups. Although we are unable to calculate the $^4J_{MeH}$ coupling constant, it is clear that the signals are less broad than the corresponding ones in **1**, which is consistent with the removal of the coupling between the aromatic protons and the *p*-Me group.

Reinforcement of the assignments and unequivocal identification of pairs of methyl groups or aromatic protons belonging to the same ring was made by using the saturation transfer method.[40] In this technique a chosen signal is irradiated to saturation and if a consequent intensity diminution of another peak is observed (and vice versa when the other peak is irradiated) this is interpreted as due to a site exchange of the protons giving the two signals by a dynamic process. Since in our system the dynamic process of lowest activation energy is the rotational process (see below), the saturation transfer method immediately indicates which pairs of methyl groups or of aromatic protons are on the same ring and exchange sites by rotations of the rings. An example of the method is shown in Figure 5. The methyl signals that on irradiation do not cause any intensity diminution of other methyl groups are recognized as *p*-methyl groups. The assignments of both the *p*-Me groups and the pairs of groups belonging to each ring, which is achieved by the saturation transfer method, are in full agreement with the assignments made by the other methods above.

Table IV shows the effect of various solvents on the chemical shifts of the various groups. The assignment of the different peaks

(40) Forsén, S.; Hoffman, R. A. *J. Chem. Phys.* **1963**, *39*, 2892; **1964**, *40*, 1189; *Acta Chem. Scand.* **1963**, *17*, 1787.

Table V. ASIS of 1 in Several Aromatic Solvents

proton(s)	C_6D_6	$C_6D_5CD_3$	C_6D_5Br	$C_6D_5NO_2$
α-*o*-Me	−0.15 (−0.16)	−0.11	−0.06	−0.05
α-*o*-Me	−0.08	−0.05	−0.03	−0.11
β′-*o*-Me	−0.11	−0.07	−0.04	+0.01
β′-*o*-Me	−0.01	0.0	−0.01	−0.07
β-*o*-Me	−0.15	−0.11	−0.07	−0.04
β-*o*-Me	−0.20	−0.15	−0.11	−0.12
α-*p*-Me	+0.18 (+0.17)	+0.17	+0.14	+0.07
β′-*p*-Me	+0.12	+0.11	+0.05	+0.02
β-*p*-Me	+0.14	+0.15	+0.13	+0.06
α-Mes H	+0.14	+0.17	+0.20	+0.22
α-Mes H	+0.05	0.0	+0.06	+0.01
β′-Mes H	+0.10	+0.12	+0.09	+0.10
β′-Mes H	+0.13	+0.04	+0.08[b]	+0.04
β-Mes H	0.0	+0.05	+0.08	+0.09
β-Mes H	0.01	+0.03	+0.02	−0.04

[a] ASIS = δ($CDCl_3$) − δ(aromatic solvent). [b] Assumed value.

in each solvent is based on the saturation transfer method and on comparison of the spectra of **1** with that of a 1:1 *E,Z* mixture of the β-mesityl-*methyl-d*$_9$ derivatives **16**.[41] The best resolution

2,4,6-$(CD_3)_3C_6H_2C$(Mes)=C(OH)Mes
16

of the signals of **1** was obtained in $C_6D_5NO_2$. The solvent effects are composed of the specific solvent–solute interactions that are accompanied by conformational changes (e.g., of the OH group or of torsional angles of the aryl groups) induced by the solvent.

Aromatic-solvent-induced shifts (ASIS)[42] are defined as ASIS = $\Delta = \delta_{CDCl_3} - \delta_{aromatic\ solvent}$ and arise from the shielding/deshielding influences of the aromatic ring current. It was originally assumed that on the average the aromatic solvent orients itself with its π cloud facing the positive region of the solute and shielding results, whereas the other part of the solute molecules will undergo an upfield or a downfield shift depending on their relative position in respect to the π cloud. However, the interpretation is complicated by the observation that the generally used "inert" internal standard Me_4Si also undergoes the ASIS phenomenon.[43] Indeed, δ(Me_4Si) is altered by 0.333 ppm in $CDCl_3$ and by 0.147 ppm in C_6D_6 with respect to external Me_4Si, i.e., the ASIS of Me_4Si is −0.48 ppm. This value is larger than most of the values reported, and it seems that there is no authentic example of an ASIS deshielding.

The relative ASIS values of Table V are based on internal Me_4Si and are uncorrected. However, a valuable comparison, which circumvents this limitation, is that of the relative shifts of protons in the same molecule. The general trend observed is that the upfield shift decreases in the order *p*-Me > Ar-H > *o*-Me, i.e., the closer is a proton of a certain ring to the double bond, the lower is its upfield shift.

The total solvent effect on nuclear shielding can be expressed as a sum of five contributions (eq 5).[44] These are the medium's

$$\sigma(\text{solvent}) = \sigma_B + \sigma_W + \sigma_A + \sigma_E + \sigma_H \qquad (5)$$

magnetic susceptibility (σ_B), the van der Waals forces between solvent and solute molecules (σ_W), the magnetic anisotropy in the solvent molecules (σ_A), the effect of an electron field on the nuclear shielding (σ_E), and the specific solute–solvent interactions, such as hydrogen bonding (σ_H). In internal comparison of the ASIS values σ_B vanishes, while σ_E and σ_H should be small for solvents such as $CDCl_3$ and C_6D_6.

(41) In the ^{1}H NMR spectrum of a 1:1 *E,Z* mixture of **16** each of the methyl groups on the β and β′ rings appears with half intensity.

(42) (a) Laszlo, P. *Progr. NMR Spectrosc.* **1967**, *3*, 231. (b) Ronayne, J.; Williams, D. H. *Annu. Rev. NMR Spectrosc.* **1969**, *2*, 83.

(43) Rummens, F. H. A.; Krystynek, R. H. *J. Am. Chem. Soc.* **1972**, *94*, 6914.

(44) Buckingham, A. D.; Schaefer, T.; Schneider, W. G. *J. Chem. Phys.* **1960**, *32*, 1227; *Ibid.* **1961**, *34*, 1064.

A general trend observed for polysubstituted benzenes is that the greater the steric congestion around the proton, the more negative is the ASIS value (using an internal standard).[45] This could be rationalized by assuming that steric hindrance of solvent approach to a solute proton affects more the protons of the internal reference by the σ_A and/or the σ_W terms than the sterically hindered proton of interest. Hence, the hindered proton will show an apparent downfield shift. Consequently, the ASIS value, combined with evaluation of the steric environments of the various protons by using space-filling models, can assist in the remaining missing assignment, i.e., in determining which protons belong to the β or to the β' ring, respectively. The nine methyl groups in **1** are exposed to environments of different crowding. The three signals that show a large positive ASIS (C_6D_6) values of +0.18, +0.12, and +0.14 are assigned to the obviously less crowded *p*-methyl group. The space-filling models show that of the six *o*-methyl groups the least crowded belongs to the β' ring and lies closer to the OH group. The corresponding signal which should show the less pronounced apparent negative ASIS value is that with an ASIS value of −0.01. Hence, the peak at $\delta(CDCl_3)$ 2.61 ppm is assigned to this methyl, which in turn also assigns the β' ring.

The models also show that the methyl groups on the β ring are more crowded and should therefore display the larger apparent downfield shifts. Indeed, the *o*-Me groups, which according to the above assignment belong to the β ring, show ASIS values of −0.15 and −0.20, which are the larger apparent negative values observed for a pair of signals.

The aromatic protons should display an ASIS pattern reminiscent of the methyls. In this way, the pair of signals with less positive ASIS values (0.00 and 0.01) are assigned to the β ring.

Table V gives ASIS values for some other solvents. A new method for comparing ASIS effects of various solvents with those of benzene was recently introduced.[46] Plots of the ASIS values for an aromatic solvent against those for C_6D_6 were found mostly to be linear, and the slopes were interpreted as a measure of the ASIS effect of the aromatic solvent. For example, for *p*-$Me_2NC_6H_4COOCH_2Me$ the slopes were 0.57, 0.12, and 0.45 in C_6H_5F, $C_6D_5NO_2$, and C_5D_5N, respectively. Deviations of a point from linearity can be ascribed to an interaction of the proton considered with the solvent that differs from those of other protons.

By plotting the data of Table V in this way we obtained linear plots for $C_6D_5CD_3$ (slope 0.8; $r = 0.95$) and C_6D_5Br (slope 0.6; $r = 0.97$, excluding one point for the α-Mes−H). Interestingly, for $C_6D_5NO_2$ we obtained two well-separated lines with slopes of 0.8 ($r = 0.91$) and 0.95 ($r = 0.99$). The points defining the latter line are those for the more crowded methyl groups at $\delta(CDCl_3)$ 1.83, 1.85, 1.86, and 1.86 ppm and for one α-Mes−H proton and one β'-Mes−H at $\delta(CDCl_3)$ 6.59 and 6.61 ppm. We found no precedent for such behavior, and at present we have no explanation for it.

Related to the ASIS are the lanthanide-induced NMR chemical shifts.[47] The use of an optically active lanthanide shift reagent is expected to shift the different signals to different degrees and to split the peaks into signals for each of the two enantiomers. However, by adding tris[3-((trifluoromethyl)hydroxymethylene)-*d*-camphorato]europium(III) to **1** in $CDCl_3$ the spectrum remained unchanged. This lack of effect is ascribed to steric hindrance to complexation of the two bulky reagents.

Several features of the ^1H NMR spectrum are noteworthy. (i) The signals for the three *p*-Me groups appear together near the position of the methyl signal of mesitylene itself.[48] This is expected since these methyl groups are the farthest from the asymmetric molecular environment, and electronic and anisotropic influences of the double bond and the other aryl groups should be sensed less in the para position. Indeed, when one of the *p*-Me groups on the β or the β' ring is replaced by a *tert*-butyl group, the $\Delta\delta = (\delta\beta_{p\text{-R}} - \delta\beta'_{p\text{-R}})$ values for R = Me and *t*-Bu are similar (0.11 and 0.13 ppm, respectively).

Table VI. ^{13}C NMR of 1 in $CDCl_3$ at Room Temperature

δ	assignment	δ	assignment	δ	assignment
20.51	α-*o*-Me[a]	128.85	α-Mes C-H[e,f]	136.68	β′-Mes *p*-*C*-Me[b]
20.64	β-Me	129.29	β-Mes C-H	137.30	α-Mes *p*-*C*-Me[e]
20.79	β′-*p*-Me[b]	129.49	β′-Mes C-H[d]	137.58	α-Mes *o*-*C*-Me[e,f]
20.93	α-*p*-Me[a,c]	129.57	α-Mes C-H[e,f]	137.92	β-Mes *C*-Me
20.97	β′-*o*-Me[d]	130.01	β-Mes C-H	138.24	β-Mes *C*-Me
21.40	β-Me	130.64	β′-Mes C-H[d]	138.47	α-Mes *o*-*C*-Me[e,f]
21.62	β-Me	132.43	α-ipso-C[e]	138.56	β′-Mes *C*-Me[d]
21.98	β′-*o*-Me[d]	133.75	β- or β′-ipso-C	139.62	β′-Mes *C*-Me[d]
22.26	α-*o*-Me[a]	134.69	β- or β′-ipso-C	148.77	C_α
114.55	C_β	135.31	β-Mes C-H		

[a] Absent in 13. [b] Absent in 15. [c] Absent in 14. [d] Shifted in 15. [e] Broadened in 13. [f] Shifted in 14.

(ii) Four of the six *o*-Me groups are shifted upfield and the remaining two are shifted downfield compared with the *p*-Me groups and the methyl groups of mesitylene in $CDCl_3$. Inspection of space-filling models indeed shows that in the frozen conformation the different *o*-Me groups are in different relationships to the neighboring aryl groups. The *o*-Me group of the α ring, which is close to the OH group, is almost in the plane of the β-aryl group and slightly above the plane of the β' ring and hence in their combined deshielding range. The combined ring-current effects are therefore deshielding, fitting the assignment for the signal at 2.43 ppm. The other *o*-Me group of the α ring is nearly in the plane of the β' ring but is above carbons 1 and 2 of the β ring. The overall shielding effect is reflected in the appearance of the signal at 1.88 ppm. Similar effects are encountered by the *o*-Me groups of the β' ring. One group is at the intersection of the planes of the two other rings and is therefore the most deshielded one at 2.61 ppm. The other *o*-Me is slightly above the plane of the β ring and is therefore shielded and absorbs at 1.85 ppm. Each of the *o*-Me groups of the β ring is above at least one carbon of one of the other two rings, respectively. The two methyls are therefore shielded and at nearly identical molecular environments and absorb at 1.83 and 1.86 ppm.

(iii) The pattern of the aromatic protons is reminiscent of that of the methyl signals. Two pairs of well-separated signals are at relatively low field, and one pair of closer signals is at a relatively high field. The symmetry properties of the Me groups in relation to the hydrogens suggests that hydrogens and methyls that are only slightly shifted belong to the same, i.e., β, ring. This is corroborated by the spectra of the analogues **15**.

The OH group of **1** may adopt either the *syn* or the *anti* conformation in relation to the double bond (cf. **1**-*syn* and **1**-*anti*).

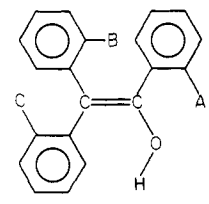

1-*syn*

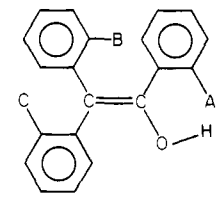

1-*anti*

In the solid state the conformation is **1**-*syn*.[13] In our solvents the OH signal appears as a sharp singlet and comparison with other enols for which the conformation may be deduced from coupling constants indicates that in the solvents used in the present work the syn conformation also predominates,[26] and any **1**-*syn* ⇌ **1**-*anti* interconversion is fast on the NMR time scale.

^{13}C NMR Spectra. The proton noise-decoupled ^{13}C NMR spectra of **1** in $CDCl_3$ at room temperature displays separate signals for each of the 29 carbons, with considerable overlap for only two of them at 20.93 and 20.97 ppm (Table VI). It indicates again a frozen conformation and hindered rotation on the NMR

(45) Williams, D. H.; Ronayne, J.; Wilson, R. G. *Chem. Commun.* **1967**, 1089.
(46) Dean, F. M.; Varna, R. S. *Tetrahedron* **1982**, *38*, 2069.
(47) (a) "Nuclear Magnetic Resonance Shift Reagents"; Sievers, R. E., Ed.; Academic Press: New York, 1973. (b) Kime, K. A.; Sievers, R. E. *Aldrichimica Acta* **1977**, *10*, 54.
(48) Acrivos, J. V. *Mol. Phys.* **1962**, *5*, 1.

Table VII. Coalescence Data for 1 in $C_6D_5NO_2$

process	$\Delta\nu$, Hz	T_c, K	$\Delta G_c^{\ddagger}$ kcal mol^{-1}
c ⇌ $\bar{d}$	10.5[a]	351.6	18.5
	31.6[b]	367.4	18.5
e ⇌ $\bar{f}$	83.7[a]	376.3	18.3
a ⇌ $\bar{b}$	60.1[a]	376.3	18.5
β-Mes H ⇌ $\overline{\beta\text{-Mes H}}$	15.7[a]	351.6	18.2
	47.0[b]	370.2	18.4
β- or β′-*C*-Me ⇌ $\overline{\beta\text{- or }\beta'\text{-}C\text{-Me}}$	21.9[c]	361[d]	18.5

[a] At 100 MHz (^{1}H). [b] At 300 MHz (^{1}H). [c] At 75 MHz (^{13}C). [d] Less accurate temperature (cf. ref 53).

time scale. The nondecoupled spectrum of **1** is very complex and no coupling constant could be deduced. The only two signals that remained as singlets were assigned to C_α and C_β of the double bond, respectively. The δ value for C_α (148.77 ppm) is similar to 149.0 ppm found by Capon et al. for C_α of vinyl alcohol,[6b] which was the only value hitherto available for an HO-bound carbon of a simple enol. However, C_β of **1** (114.55 ppm) appears at a lower field than C_β of vinyl alcohol (94.4 ppm). The lack of apparent coupling for C_α indicates that $^2J_{=COH} < 2$ Hz.

Assignment of the signals was based on comparison of the spectra of **1** and its derivatives **13–15** at the same temperature, pulse width, and pulse delay. The three methyl signals at δ 20.51, 20.93, and 22.26, which are absent in the spectrum of **13**, were assigned as belonging to the α-mesityl ring since the intensity of a CD_3 signal should strongly diminish (and it may even disappear) due to the longer relaxation time, the splitting to seven peaks, and the diminution of the nuclear Overhauser effect.[49] Similarly, the six signals in the aromatic region with reduced intensities in the spectrum of **13** were assigned to the α-mesityl ring carbons.

Off-resonance irradiations (^{1}H irradiations at Me_4Si frequency, 20 W, attenuations of 11, 20, and 25 dB) afforded additional information. At 11 dB all the signals were unaffected except for widening and concomitant intensity reduction of six consecutive signals at δ 128.85–130.64. Since the methyl protons are completely saturated whereas the aromatic protons are only partially saturated, these signals are due to the aromatic carbons directly attached to protons (Ar*C*–H). The corresponding carbons in mesitylene appear at 127.2 ppm.[50] At 20 dB broadening of the six signals was extensive and they "coalesce" to a single peak. At 25 dB the six signals began to show coupling, three other signals at 132.43, 133.75, and 134.69 ppm began to broaden, and the nine remaining signals at a lower field were unaffected. The three signals were ascribed to the ipso carbons of the mesityl rings and the nine signals at 135.31–139.62 ppm to the methyl-substituted carbons. The corresponding value in mesitylene is 137.5 ppm.[50]

The assignment of the α-ring methyl groups as ortho or para was based on comparison with the spectra of **14** and of the β- and β′-ring methyl groups on comparison with the spectra of either the equilibrium **15a–15b** mixture or of a mixture enriched by **15a**.

Dynamic Stereochemistry. The best resolved spectra of **1** are obtained in $C_6D_5NO_2$, and since this solvent also allows work at high temperature it was the solvent mostly used in the DNMR work. On raising the temperature of a solution of **1** in $C_6D_5NO_2$ 12 proton signals start to broaden and finally coalesce. The unchanged signals are those previously assigned for the *p*-Me groups and the OH. Working at 100 MHz, three coalescence processes can be followed in the methyl region with coalescence temperatures at the range of 351.6 (α-*o*-Me) to 376.3 K (β- and β′-*o*-Me). Similarly we measured one coalescence process in the aromatic region. The experiment was repeated at 300 MHz where the coalescence of the β-*o*-Me groups and of the β-Mes-H protons were measured. The data are given in Table VII. The T_c values for the coalescence of the α- and the β′-Me are considered to be less accurate due to the difficulties in distinguishing separate coalescence temperatures.

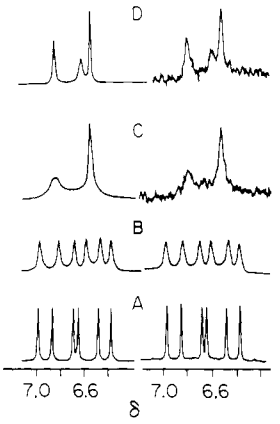

Figure 6. Experimental (left) and calculated (right) spectra of the aromatic region of **1** in $C_6D_5NO_2$. A: at 288 K (300 MHz); B: at 367 K (300 MHz); C: at 376 K (100 MHz); D: at 393 K (100 MHz).

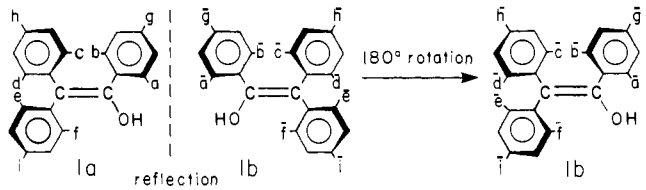

Figure 7. Relationship between the two enantiomers **1a** and **1b** and their enantiomeric sites.

In all the cases, the $\Delta\nu$ values were measured under slow-exchange conditions at 300 MHz and the value divided by 3 in order to obtain a precise $\Delta\nu$ value for use at 100 MHz. This is of great importance when $\Delta\nu$ is small (e.g., for the coalescence of the β-*o*-Me groups where $\Delta\nu$ = 10 Hz). The exchange rate at the coalescence temperature was calculated by using the Gutowsky–Holm approximation[51] ($k_c = \pi\Delta\nu/2^{1/2}$) and the $\Delta G_c^{\ddagger}$ value by using the Eyring equation, assuming a transmission coefficient of unity. Thd $\Delta G_c^{\ddagger}$ values for all the processes were very similar (Table VII) and their average value is 18.4 ± 0.1 kcal mol^{-1}.

The barrier for the coalescence of the three pairs of aromatic protons was also calculated by a total line-shape analysis.[52] The best fit between the calculated and the observed spectra (Figure 6) was obtained by assuming that the rate of exchange for the pairs of protons are identical. The $\Delta G_c^{\ddagger}$ values obtained were 18.1 ± 0.1 kcal mol^{-1}.

At 423 K fast exchange occurs and five sharp signals in the methyl region (1.98, 2.09, 2.15, 2.27, and 2.32 ppm for 2 β-*o*-Me, β-*p*-Me, α-*p*-Me, β′-*p*-Me + 2 α-*o*-Me, 2 β′-*o*-Me, respectively), three sharp signals in the aromatic region (6.63, 6.71, and 6.91 ppm for the 2 β-, 2 α- and 2 β′-mesityl-H), and a sharp OH singlet at 5.21 ppm are observed. It is noteworthy that the OH signal shifts by <0.3 ppm on raising the temperature from 293 to 423 K. When the sample was cooled to room temperature the 16-signal spectrum of **1** reappeared without any traces of decomposition products. When a solution of **1** in acetone-d_6 was cooled to 203 K the OH signal remained sharp and no possible splitting due to the separate syn- and anti-OH signals was observed.

The coalescence study in $C_6D_5NO_2$ was repeated when 1 drop (0.05 mL) of CF_3COOH was added to the NMR tube. The spectra during the coalescence processes were found to be identical in the presence and the absence of the acid and the same T_c values were obtained.

(49) Abraham, R. J.; Loftus, P. "Proton and Carbon-13 NMR Spectroscopy, an Integrated Approach"; Heyden: London, 1978; p 146.
(50) Breitmaier, E.; Woelter, W. "^{13}C NMR Spectroscopy"; Verlag-Chemie: Weinheim, 1978; p 185.
(51) Gutowsky, H. S.; Holm, C. H. *J. Chem. Phys.* **1956**, *25*, 1228.
(52) The program used was program CLATUX which was applied to each of the several pairs of exchanging groups (Binsch, G. *Top. Stereochem.* **1968**, *3*, 97). Since use of the approximate Gutowsky–Holm equation gave identical results, we used this equation for calculating the other $\Delta G_c^{\ddagger}$ values. For a discussion of the validity of the approximation, see: Kost, D.; Carlson, E. H.; Raban, M. *Chem. Commun.* **1971**, 656.

Table VIII. Chemical Shifts and Assignments for Compounds 14, 18, 19, 20, and 25 in $CDCl_3$ and in the Coalescence Solvent[a]

	compound									
	14		18		19		20		25	
	solvent									
assignment	$CDCl_3$	1,2,4-$C_6H_3Cl_3$[b]	$CDCl_3$[c]	1,2,4-$C_6H_3Cl_3$[b,d]	$CDCl_3$[e]	$C_6D_5NO_2$[f]	$CDCl_3$	$C_6D_5CD_3$	$CDCl_3$[g]	$C_6D_5NO_2$[h]
α-*o*-Me	1.92	1.99	1.95	2.04	1.86	1.93	1.96	2.06		
α-*o*-Me	2.42	2.50	2.32	2.39	2.35	2.50	2.51	2.60		
β-*o*-Me	1.84	1.90	1.84	1.89	1.75	1.93	1.91	2.04	1.46	1.65
β-*o*-Me	1.86	1.93	1.88	2.00	1.89	2.00	1.96	2.10	2.11	2.21
β'-*o*-Me	1.84	1.90	1.84	1.89	1.87	1.90	1.91	2.00	1.93	1.92
β'-*o*-Me	2.60	2.70	2.50	2.59	2.59	2.68	2.66	2.79	2.84	2.95
α-*p*-Me			2.20	2.08	2.22	2.11	2.21	2.00		
β-*p*-Me	2.12	2.08	2.15	2.06	2.11	2.06	2.13	1.93	1.92	1.76
β'-*p*-Me	2.27	2.27	2.25	2.23	2.25	2.21	2.27	2.17	2.33	2.28
OH	5.31								5.70	5.92
α-Mes H	6.73 (m)		6.63		6.60	6.47	6.60	6.39		
α-Mes H	7.03 (2 H, m)		6.81		6.83	6.63	6.88	6.76		
β-Mes H	6.57		6.58		6.50	6.45	6.57	6.47	6.17	6.11
β-Mes H	6.63		6.63		6.57	6.89	6.61	6.54	6.54	6.57
β'-Mes H	6.81		6.73		6.69	6.47	6.74	6.65	6.89	6.76
β'-Mes H	7.05		6.92		6.92	6.95	6.97	6.93	7.12	7.07

[a] Unless otherwise stated the Me and the Mes H protons are singlets with the appropriate integration. [b] The OH and the aromatic protons are covered by the solvent signals. [c] δ OCOMe 1.88. [d] δ OCOMe 1.80. [e] δ $CHMe_2$ 0.93, 1.11; $CHMe_2$ 3.83. [f] δ $CHMe_2$ 0.91, 1.02; $CHMe_2$ 3.88. [g] δ 9-anthryl H 7.21 (2 H, m), 7.47 (2 H, m), 7.80 (1 H, d), 7.97 (1 H, d), 8.30 (1 H, d), 8.37 (1 H, s), 8.55 (1 H, d). [h] δ 9-anthryl H 7.10 (1 H, t), 7.25 (1 H, t), 7.53 (1 H, t), 7.63 (2 H, m), 8.07 (1 H, d), 8.36 (1 H, s), 8.53 (1 H, d), 8.81 (1 H, d).

A DNMR experiment was also conducted by monitoring the ^{13}C signals in $C_6D_5NO_2$. The assignment of the signals required for this study was achieved by comparison with the assignment given in Table VI in $CDCl_3$ and with the spectrum of **13**. Due to the large $\Delta\nu$ values for most of the pairs of the diastereotopic carbon signals most of the coalescence temperatures were beyond the accessible range of the instrument, and only one coalescence process could be unequivocally followed. This involved either the pair of β or β'-Mes *C*-Me carbons, which absorb at room temperature at 138.50 and 138.79 ppm and coalesce at 361 K.[53] The barrier calculated for this process is 18.5 kcal mol^{-1}, which is in agreement with the barrier obtained from the ^1H NMR spectrum.

Processes Leading to Coalescence. In order to analyze the different processes that lead to coalescence we draw in Figure 7 the two enantiomers of trimesitylethenol, i.e., **1a** and **1b**, as mirror images. We label the positions of the methyl groups in **1a** by the letters a–i, and the groups in enantiomeric sites in **1b** are labeled by the same letters with an overbar (i.e., ā–ī). The conventional drawing of **1b**, with OH at the bottom right, is obtained by rotation of the mirror image of **1a** by 180°. Each pair of groups that is site exchanged as a result of a particular stereoisomerization process is given in a single bracket, and the overall change is indicated by the sets of brackets for the various pairs.

The observed coalescence of several or all the pairs of signals can a priori be achieved by a multitude of nonflip and flip processes. The nonflip routes involve rotation around the C_α–C_β double bond (eq 1) and ketonization to trimesitylethanone **17**

$$Mes_2CHCOMes$$
17

followed by enolization (eq 3), reactions initiated by initial ionization (Scheme I) and 180° (π-radians) rotation of the three rings by a concerted or a nonconcerted mechanism without concomitant helicity reversal. The flip mechanisms are discussed below.

Exclusion of Nonflip Routes. The nonflip processes are excluded by the following arguments. (a) The analysis of the rotation around the double bond shows that it leads to the (aa)(bb)(cf)(de)(ed)(fc)(hi)(ih)(gg) permutation. Consequently, it will lead to coalescence of the *p*-methyl groups of the β and the β' ring. Above the coalescence temperature six methyl signals (2 *p*-Me and 4 *o*-Me) should be observed. Even when this process is coupled with π-radians rotation of the α ring it should lead to five methyl signals (2 *p*-Me, 3 *o*-Me). Since the three *p*-methyl signals remain anisochronous at 473 K, which is well above the coalescence temperature of the *o*-Me signals (i.e., the six signals at 473 K are three ortho and three para signals), no (hi)(ih) interchange takes place, and this route is therefore excluded. The barrier to the (hi)(ih) interchange should be higher than 25 kcal mol^{-1}, which is consistent with our success in enriching the isomer mixture of **15a** and **15b** by **15a** by applying fractional crystallization from EtOH at room temperature.

(b) The ketonization–reenolization route of eq 3 or the analogous acid-catalyzed process is excluded by several lines of evidence. First, the ketone **17** could not be prepared either directly,[9c] or by ketonization of **1**. It could be argued that the low thermodynamic stability of **17** does not exclude a rapid (kinetic) ketonization–enolization process, but both the ketonization and the enolization of closely related systems, as in the reaction of eq 6, are slow even at 323 K.[26] Moreover, the NMR spectra of

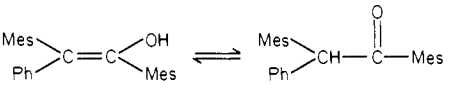

(6)

mixtures of ketones and enols usually show signals for both species,[54] so that their interconversion is slow on the NMR time scale. Second, the coalescence temperature does not decrease appreciably on addition of CF_3COOH—a relatively strong acid. In this case it could be expected that either the ionization of **1** to the enolate ion will be inhibited, resulting in a decrease in the enantiomerization rate, or that the intrusion of an acid-catalyzed ketonization route will increase the enantiomerization rate. Finally, since this route is impossible for $Mes_2C{=}C(X)Mes$ derivatives where $X \neq OH$, we prepared trimesitylvinyl acetate (**18**),

$Mes_2C{=}C(OAc)Mes$ **18** $\quad$ $Mes_2C{=}C(OCHMe_2)Mes$ **19**

$Mes_2C{=}C(Cl)Mes$ **20** $\quad$ $Mes_2C{=}C(OAc)C_6H_3Me_2$-2,6 **21**

isopropyl ether (**19**), and chloride (**20**) and α-(2,6-dimethylphenyl)-β,β-dimesitylvinyl acetate (**21**) and compared their coalescence behavior with those of **1**. The acetate **18** was prepared by Fuson's method,[9c] and the pairs of signals involved in the

(53) This temperature is believed to be less accurate than the temperatures measured in the ^1H DNMR experiments. This is due to the heat produced by the strong irradiation of the protons, and since the temperature was measured in this case with a thermocouple.

(54) Kol'tsov, A. I.; Kheifets, G. M. *Russ. Chem. Rev.* (*Engl. Transl.*) **1971**, *40*, 773.

Table IX. Coalescence Data for $Mes_2C{=}C(X)Ar$ Derivatives[a]

compd	Ar	X	solvent	process[b]	$\Delta\nu$, Hz	T_c, K	$\Delta G_c^{\ddagger}$, kcal mol^{-1}	
1	Mes	OH	1,2,4-$C_6H_3Cl_3$	c $\rightleftharpoons$ $\overline{\text{d}}$	1.3	325.8	18.3[c]	
				a $\rightleftharpoons$ $\overline{\text{b}}$	60	378.3	18.5[c]	18.4 ± 0.1[e]
				e $\rightleftharpoons$ $\overline{\text{f}}$	79	378.3	18.3[c]	
14	2,6-$Me_2C_6H_3$	OH	1,2,4-$C_6H_3Cl_3$	c $\rightleftharpoons$ $\overline{\text{d}}$	3	336.8	18.4[c]	
				a $\rightleftharpoons$ $\overline{\text{b}}$	51	386.3	19.1[c]	18.7 ± 0.2[e]
				e $\rightleftharpoons$ $\overline{\text{f}}$	80	386.3	18.7[c]	
18	Mes	OAc	1,2,4-$C_6H_3Cl_3$	c $\rightleftharpoons$ $\overline{\text{d}}$	11	367.9	19.2[c]	
				a $\rightleftharpoons$ $\overline{\text{b}}$	34	383.3	19.2[c]	19.0 ± 0.2[e]
				e $\rightleftharpoons$ $\overline{\text{f}}$	71	383.3	18.7[c]	
19	Mes	$OCHMe_2$	$C_6D_5NO_2$	c $\rightleftharpoons$ $\overline{\text{d}}$	19.2	312.3	16.0	
				a $\rightleftharpoons$ $\overline{\text{b}}$	158.5	336.9	15.9	
				e $\rightleftharpoons$ $\overline{\text{f}}$	234.4	336.9	15.6	
				β-Mes H $\rightleftharpoons$ $\overline{\text{β-Mes H}}$	54.8	321.7	15.8	15.8 ± 0.1[e]
				α-Mes H $\rightleftharpoons$ $\overline{\text{α-Mes H}}$	126.8	331.8	15.8	
				β′-Mes H $\rightleftharpoons$ $\overline{\text{β′-Mes H}}$	143.6	331.8	15.7	
				CH*Me*Me $\rightleftharpoons$ $\overline{\text{CHMe*Me*}}$	36.6	318.1	15.9	
20	Mes	Cl	$C_6D_5CD_3$	c $\rightleftharpoons$ $\overline{\text{d}}$	19.5	321.9	16.5	
				a $\rightleftharpoons$ $\overline{\text{b}}$	160.3	348.5	16.4	
				e $\rightleftharpoons$ $\overline{\text{f}}$	238.6	348.5	16.2	
				β-Mes H $\rightleftharpoons$ $\overline{\text{β-Mes H}}$	21.0	321.9	16.4	16.4 ± 0.1[e]
				α-Mes H $\rightleftharpoons$ $\overline{\text{α-Mes H}}$	109.6	341.0	16.3	
				β′-Mes H $\rightleftharpoons$ $\overline{\text{β′-Mes H}}$	84.9	339.6	16.4	
21	2,6-$Me_2C_6H_3$	OAc	1,2,4-$C_6H_3Cl_3$	c $\rightleftharpoons$ $\overline{\text{d}}$	6	359.6	19.2[c]	
				a $\rightleftharpoons$ $\overline{\text{b}}$	34	385.2	19.3[c]	19.1 ± 0.2[e]
				e $\rightleftharpoons$ $\overline{\text{f}}$	67	385.2	18.8[c]	
25	9-anthryl	OH	$C_6D_5NO_2$	c $\rightleftharpoons$ $\overline{\text{d}}$	56.1	329.2	16.1[c]	
				e $\rightleftharpoons$ $\overline{\text{f}}$	102.5	344.5	16.4[c]	
				β-Mes H $\rightleftharpoons$ $\overline{\text{β-Mes H}}$	137.1	342.8	16.2	16.2 ± 0.1[e]
				β′-Mes H $\rightleftharpoons$ $\overline{\text{β′-Mes H}}$	94.2	337.5	16.2	
				peri-Anth H $\rightleftharpoons$ $\overline{\text{peri-Anth H}}$	86.4	332.1	16.0	
				peri-Anth H $\rightleftharpoons$ $\overline{\text{peri-Anth H}}$	118.5	337.5	16.0	

[a] At 300 MHz. [b] The enantiomeric process is not shown. [c] At 100 MHz. [d] Less accurate value. [e] Average value.

coalescence processes were identified by comparison with the spectrum of **1** and by the saturation transfer technique. The chemical shifts and assignments are given in Table VIII, and the presence of two configurations at low temperature is discussed below. The ether **19** and the chloride **20** are also discussed below in connection with other possible enantiomerization routes, and their spectra and assignments are given in Table VIII. Several coalescence processes of the methyl groups and the aromatic protons were measured for each compound, and the data that are given in Table IX show two clear features: (i) In each case the $\Delta G_c^{\ddagger}$ values for the coalescences of pairs of signals in the three rings are nearly the same, i.e., a correlated process of the three rings is highly likely. (ii) The $\Delta G_c^{\ddagger}$ values for the four compounds are not drastically different and those for **18** and **1** are nearly identical under similar conditions: e.g., $\Delta G_c^{\ddagger}$(1,2,4-$C_6H_3Cl_3$) = 19.0 ± 0.2 and 18.4 ± 0.1 kcal mol^{-1}, respectively. Hence, any mechanism that ascribes a specific role to the enolic hydrogen, such as ketonization, is excluded.

(c) Reversible S_N1 ionization of **1** to form a vinyl cation is unlikely due to the low nucleofugality of the OH group. However, since an α-mesityl group is a good activator in vinyl cation formation[55] and bulky β-aryl groups will increase the ionization rate by steric enhancement,[22] this route cannot be excluded unequivocally on this basis. However, comparison with the data of Table IX for **18** and especially for **20** excludes this route. Acetate, and especially chloride, will be much better leaving groups than OH in an S_N1 process, and the nearly identical $\Delta G_c^{\ddagger}$ values for **1** and **18** and even the somewhat lower $\Delta G_c^{\ddagger}$ value for **20**, suggest a similar mechanism. The activation energies for the C–X bond cleavage should be much more different. Nevertheless, this process may be observable when X is a supernucleofuge such as a triflate OSO_2CF_3.

A catalyzed S_N1 process, which proceeds at a much slower rate than the coalescence rate, is probably involved in the preparation of the chloride **20** from **1** and $SOCl_2$ in the presence of a catalytic amount of pyridine (eq 7). The reaction was complete after 5

$$\underset{\mathbf{1}}{Mes_2C{=}C(OH)Mes} \xrightarrow[C_6H_5CH_3]{SOCl_2,\ pyridine} \underset{\mathbf{20}}{Mes_2C{=}C(Cl)Mes} \qquad (7)$$

h at room temperature. This conversion is believed to occur in sp^3-hybridized and allylic systems by the ion pair mechanism of eq 8.[56] Indeed, when the reaction was performed with the α-

$$ROH + SOCl_2 \rightarrow R^+\ {}^-OSCl(=O) + HCl \rightarrow RCl + SO_2 \qquad (8)$$

ring-methyl-deuterated analogue **13**, the chloride **20** was formed with an almost statistical distribution of the label at the three positions.[26] Since the three aryl rings are identical, except for isotopic labeling, this is an example of the ionization–rearrangement–recombination (with other nucleophile) route.

(d) Several rotational mechanisms can lead to coalescence with topomerization but without helicity reversal and enantiomerization. They are given in Table X under the heading "nonflip". For example, a correlated rotation of the three rings by 180° would result in the (ab)(ba)(cd)(dc)(ef)(fe) permutation, i.e., it will give coalescence of three pairs of *o*-Me groups, but without helicity reversal. Likewise, three consecutive rotations by 180° of the α, β, and β′ rings ([α], [β], [β′]) will give the same result. Nonflip mechanisms of this type were excluded by Mislow for systems **3** and **4**,[18] and we excluded them previously as the threshold mechanisms in our system by analogy.[1a] An unequivocal exclusion of these routes is obtained by substitution of our system with an appropriate enantiomerization probe, as discussed below.

The Possible Flip Mechanisms. Evidence for the Three-Ring Flip. By elimination of alternatives the most probable coalescence route involves rotation around the C(sp^2)–C(Ar) bonds. The similar $\Delta G_c^{\ddagger}$ values for the constitutionally different aryl rings

(55) Yates, K.; Pĕriĕ, J. J. *J. Org. Chem.* **1974**, *39*, 1902.

(56) March, J. "Advanced Organic Chemistry", 2nd ed.: McGraw-Hill: New York, 1977; p 302.

Table X. Sites Exchanged by Flip and Nonflip Rotational Routes for **1a**[a]

ring flip route	flipping[b] rings	flip	rotating[c] rings	nonflip
zero ring	[0]	(aā)(bb̄)(cc̄)(dd̄)(eē)(ff̄)(gḡ)(hh̄)(ii)	[0]	(a)(b)(c)(d)(e)(f)(g)(h)(i)
one ring	[α]	(ab̄)(bā)(cc̄)(dd̄)(eē)(ff̄)(gḡ)(hh̄)(ii)	[α]	(ab)(ba)(c)(d)(e)(f)(g)(h)(i)
	[β]	(aā)(bb̄)(cd̄)(dc̄)(eē)(ff̄)(gḡ)(hh̄)(ii)	[β]	(a)(b)(cd)(dc)(e)(f)(g)(h)(i)
	[β′]	(aā)(bb̄)(cc̄)(dd̄)(ef̄)(fē)(gḡ)(hh̄)(ii)	[β′]	(a)(b)(c)(d)(ef)(fe)(g)(h)(i)
two ring	[α,β]	(ab̄)(bā)(cd̄)(dc̄)(eē)(ff̄)(gḡ)(hh̄)(ii)	[α,β]	(ab)(ba)(cd)(dc)(e)(f)(g)(h)(i)
	[α,β′]	(ab̄)(bā)(cc̄)(dd̄)(ef̄)(fē)(gḡ)(hh̄)(ii)	[α,β′]	(ab)(ba)(c)(d)(ef)(fe)(g)(h)(i)
	[β,β′]	(aā)(bb̄)(cd̄)(dc̄)(ef̄)(fē)(gḡ)(hh̄)(ii)	[β,β′]	(a)(b)(cd)(dc)(ef)(fe)(g)(h)(i)
three ring	[α,β,β′]	(ab̄)(bā)(cd̄)(dc̄)(ef̄)(fē)(gḡ)(hh̄)(ii)	[α,β,β′]	(ab)(ba)(cd)(dc)(ef)(fe)(g)(h)(i)

[a] Letters (a–i, ā–ī) in each bracket indicate the corresponding site-exchanging groups. [b] Letters in square brackets indicate the flipping ring(s). [c] Letters in square brackets indicate the rotating ring(s).

strongly indicate that a correlated rotation is being involved; i.e., the three rings are rotating in a single geared motion.

In the analysis above we outlined that the rotations may involve both nonflip and flip mechanisms. Flip mechanisms that involve correlated rotations are the zero-, one-, two-, and three-ring flips (Figure 3). All of them involve helicity reversal and should be considered in searching for the lowest energy path for the coalescence. In the Ar_3Z series **3** and **4**, Mislow and co-workers presented strong evidence,[15-19] which is based on empirical force-field calculations[17d,e] and NMR studies,[18] that the rotational mechanism of lowest activation energy (the so-called "threshold" mechanism) is the two-ring flip. This is corroborated by recent X-ray diffraction data.[57] DNMR evidence that the threshold mechanism indeed involves helicity reversal was shown by studying the boron derivative **22**.[18] The symmetry of one of the rings in

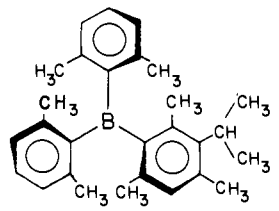

22

22 was eliminated by using the isopropyl group as an enantiomerization probe. The rotational barrier was calculated from the exchange of the methyl groups of the unsubstituted *m*-xylyl rings, whereas the presence of the *m*-isopropyl group enabled the measurement of the energy barrier for the enantiomerization (which involves helicity reversal). The observation of identical barriers for the two processes corroborated the assumption that the correlated rotation involves helicity reversal. A minor drawback in the use of **22** is that the isopropyl group renders the neighboring methyl groups constitutionally distinct, thus excluding the study of the exchange process in the unsymmetrically substituted ring.

An elegant method overcoming this problem was introduced by Binsch and co-workers[58] who monitored simultaneously the edge-interchange and helicity-reversal processes for compounds **23** and **24** by using ^{19}F NMR. In the propeller conformation the

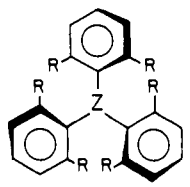

Z=P,As R=CHF_2

23

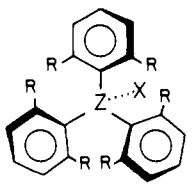

Z=P, As R=CHF_2 X=O

24

two CHF_2 groups at each ring are diastereotopic and enable one to follow the edge-interchange process. The two F atoms of each CHF_2 group are also diastereotopic since the CHF_2 group is prochiral, thus enabling one to follow the helicity-reversal process. The barriers found for the two processes were identical.

Sixteen different rotational mechanisms are possible in our system. Eight of them are flip mechanisms involving helicity reversal, and eight are nonflip mechanisms in which the rings rotate by π-radians while the nonrotating ring(s) remain fixed. The sites exchanged by these routes are summarized in Table X.

A priori, either three consecutive one-ring flips ([α], [β], [β′]), two consecutive two-ring flips (e.g., [α,β] and [β,β′]), a three-ring [α,β,β′] flip, or the equivalent combinations of "nonflip" mechanisms can account for the coalescence results. In contrast with trimesitylmethane[17b] or trimesitylboron[18] each mesityl group of **1** resides in a different molecular environment and its flip is expected to give a different $\Delta G_c^{\ddagger}$ value. If $\Delta G_c^{\ddagger}$ is mainly determined by the mutual steric interactions of both the flipping and the nonflipping rings in the ground and the transition states, it is expected that $\Delta G_c^{\ddagger}$([α]-ring flip) $\neq$ $\Delta G_c^{\ddagger}$([β]-ring flip) $\neq$ $\Delta G_c^{\ddagger}$([β′]-ring flip) and that $\Delta G_c^{\ddagger}$([α,β]-ring flip) $\neq$ $\Delta G_c^{\ddagger}$([α,β′]-ring flip) $\neq$ $\Delta G_c^{\ddagger}$([β,β′]-ring flip). *Consequently, the identical $\Delta G_c^{\ddagger}$ values for the three rings strongly indicate that a single process, most likely a three-ring flip, is involved.*

However, three problems have to be answered in order to establish unequivocally that the three-ring flip is the pathway of lowest energy. First, the nonflip coalescence routes should be excluded. Second, it should be established that the coalescence is accompanied by enantiomerization, and that the lowest energy pathway for the enantiomerization is the one that is actually measured. Third, since the chemical similarity of the three rings of **1** may result in an accidental identity of the $\Delta G_c^{\ddagger}$ values for either the three one-ring flips or the three two-ring flips, it should be shown that the same behavior is still observed when this identity is removed.

Table X shows that the zero-ring flip is the only flip route that does not exchange diastereotopic groups. Consequently, it cannot be monitored by NMR, and there is a possibility that the coalescence via the three-ring flip proceeds with enantiomerization with the observed barrier but that the zero-ring flip leads to enantiomerization with a lower barrier which is hidden in the conditions of the coalescence experiment. If only racemic **1** is available, this possibility can be excluded by two ways. First, space-filling models show that the transition state for the zero-ring flip where the three rings are simultaneously coplanar (or nearly so) with the double bond is so overcrowded that it is practically unachievable. In contrast, the transition state for the three-ring flip seems relatively much less hindered. Second, unequivocal evidence that the rotational mechanism involves helicity reversal and that the three-ring flip is the threshold mechanism is obtained by substituting **1** with an enantiomerization probe. In order to prevent a change in the local C_2 symmetry of the three rings we attached the prochiral isopropyl group to the oxygen atom.

Oxygen alkylation of **1** via its enolate under phase-transfer conditions with isopropyl bromide as both the reagent and the solvent gave the ether **19** in good yield (eq 9). The ^1H NMR

$$\underset{\mathbf{1}}{Mes_2C{=}C(OH)Mes} \xrightarrow[\text{quat}]{i\text{-PrBr/aq NaOH}} Mes_2C{=}C(O^-)Mes \xrightarrow{i\text{-PrBr}} \underset{\mathbf{19}}{Mes_2C{=}C(OCHMe_2)Mes} \quad (9)$$

(57) Bye, E.; Schweizer, W. B.; Dunitz, J. D. *J. Am. Chem. Soc.* **1982**, *104*, 5893.

(58) Wille, E. E.; Stephenson, D. S.; Capriel, P.; Binsch, G. *J. Am. Chem. Soc.* **1982**, *104*, 405.

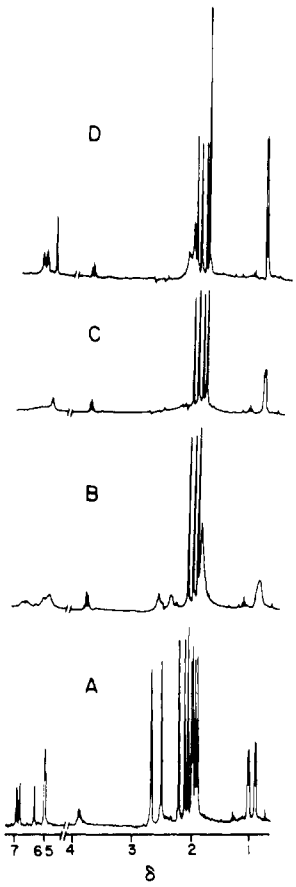

Figure 8. ^{1}H 300-MHz NMR spectrum of **19** in $C_6D_5NO_2$. A: at 277 K; B: at 318 K; C: at 337 K; D: at 373 K.

spectrum of **19** in $C_6D_5NO_2$ at 277 K (Table VIII, Figure 8) reveals an important feature. The methyl groups of the isopropyl moiety appear as two separate doublets centered at 0.91 and 1.03 ppm (J = 6.26 Hz) of equal intensity. The methine proton appears as a single septet. This is strong evidence that the molecule adopts a chiral conformation in solution, and the two diastereotopic methyl groups indicate the presence of the two species **19a** and **19b**.

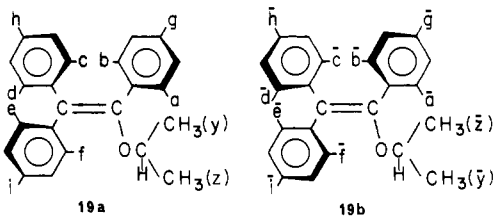

Unfortunately, although it is desirable to establish that the substitution on the oxygen does not change the geometry, we were unable so far to obtain good crystals of **19** for X-ray determination. However, the similarity in the structures of **1** and **18** (see below) in the solid state leaves little doubt that **19** also exists in a propeller conformation. For the DNMR study the signals of **19** were assigned by the saturation transfer technique and by comparison with those of **1** (Table VIII). When the temperature is raised seven coalescence processes were observed: three for the pairs of *o*-Me protons, three for the pairs of aromatic protons, and one for the two doublets of the isopropyl group, which coalesce to a single doublet (Figure 8). The $\Delta G_c^{\ddagger}$ values for the seven processes are summarized in Table IX. The most significant result is that the $\Delta G_c^{\ddagger}$ value obtained from the coalescence of the methyls of the isopropyl group is identical within the experimental error with the average value obtained for the other six coalescence processes for the three rings. Since the coalescence of the isopropyl doublets can take place only when the **19a** ⇌ **19b** enantiomerization takes place, the nonflip rotational pathways are excluded. Moreover, *the identity of the $\Delta G_c^{\ddagger}$ values for the enantiomerization (i-Pr probe) and rotation (o-Me and ArH probes) excludes enantiomerization with a lower barrier via a zero-ring flip and identifies the threshold rotational mechanism as the three-ring flip.*

Accidental identical barriers will be very unlikely if similar $\Delta G_c^{\ddagger}$ values for the three rings will be still obtained when either the molecular environment is changed when the three rings are chemically or sterically identical or when the rings become chemically and sterically nonequivalent.

A change in the molecular environment in the vicinity of the α and the β' rings is caused by a change in X. Table IX indicates that the $\Delta G_c^{\ddagger}$ values for $Mes_2C{=}C(X)Mes$, X = OH (**1**), OAc (**18**), $OCHMe_2$ (**19**), and Cl (**20**), are different, but for each compound they are identical for the three rings. The difference between the extremes, which are 15.8 kcal mol^{-1} for X = $OCHMe_2$ and 19.0 kcal mol^{-1} for X = OAc, are significant and argue strongly against the assumption of accidental identical barriers for the three rings. This conclusion will be augmented if the rings themselves will be different. Table IX shows again that a change of the α-mesityl to an α-2,6-dimethylphenyl group has no effect on the barriers when X is either OH (**1** and **14**) or OAc (**18** and **21**). This is not surprising since the steric environment around the reaction site, which is largely responsible for the magnitude of the rotational barrier, is the same for both the mesityl and the α-2,6-dimethylphenyl rings. We therefore synthesized a new crowded enol, 1-(9-anthryl)-2,2-dimesitylethenol (**25**), by the

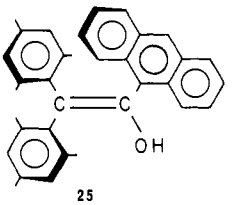

25

reaction of dimesityl ketene with 9-anthrylmagnesium bromide (cf eq 4). The α-9-anthryl group of **25** is both chemically and sterically different from the α-mesityl group of **1**, and the barriers for the rotations that involve the α-aryl group, either directly or indirectly, should be different.

X-ray diffraction data indicate that **25** also has a propeller structure in the solid state.[13] Its ^{1}H NMR at 300 MHz in $CDCl_3$ at 290 K shows 12 singlets assigned to the six methyl groups, the four Mes-H protons, H-10 of the anthryl ring, and the OH group (5.70 ppm), as well as four doublets for the four peri hydrogens (J = 8 Hz) and two multiplets for the 2-, 3-, 6-, and 7-protons of the anthryl ring. A better resolution is obtained again in $C_6D_5NO_2$ where the two multiplets appear as four distorted triplets. A frozen propeller conformation in solution is therefore highly likely.

Comparison of the spectra of **25** on the one hand and of **1**, **14**, **18**, **19**, and **20** on the other (Tables IV and VIII) shows that the $\Delta\delta$ value for the pairs of two *o*-Me or Mes-H diastereotropic protons for the β' ring (0.91 and 0.23 ppm, respectively) are similar or somewhat larger for **25**, but the $\Delta\delta$ values for the β-*o*-Me protons (0.65 ppm) and the β-Mes H protons (0.37 ppm) are much larger than the corresponding average values for the trimesitylvinyl systems (0.05 ± 0.03 and 0.06 ± 0.01 ppm, respectively). Likewise, the $\delta(\beta'$-*p*-Me)$-\delta(\beta$-*p*-Me) difference for **25** is 0.41 ppm compared with 0.14 ± 0.02 ppm for the other compounds. These differences can be traced to a large upfield shift of one β-*o*-Me and one β-Mes H proton of **25** and an accompanying relatively small downfield shift of the other β-*o*-Me and β-Mes H proton compared with the trimesitylvinyl systems. This is consistent with the increased torsional angle of the α-9-anthryl group of **25** compared with the α-mesityl group of **14**, **18**, **19**, and **20**, which brings more of the neighboring *o*-Me and aromatic H of the β-mesityl group into the shielding region of the aromatic ring, whereas the further away protons move more into the deshielding region.

Pairs of diastereotopic protons or groups were identified by the saturation transfer technique. When the temperature was raised

the corresponding signals started to coalesce and six coalescence processes were measured between 329 and 344 K. Four of them involve either the *o*-Me groups or the aromatic protons of the mesityl rings and the two others were for the two pairs of the peri-9-anthryl ring protons. The $\Delta G_c^{\ddagger}$ values (Table IX) were almost identical, being 16.2 ± 0.1 kcal mol^{-1}, thus ruling out convincingly three consecutive one-ring or two consecutive two-ring flips as plausible alternatives for the rotational mechanism.

We want to emphasize that the similar $\Delta G_c^{\ddagger}$ values for rotation of sterically and chemically different aryl rings is a direct evidence that a correlated rotation occurs. This is not the case with systems **3** and **4** where the correlated rotation phenomenon cannot be probed by coalescence studies alone. For example, in Ar_3Z systems with three identical aryl groups, the coalescence process gives only a single $\Delta G_c^{\ddagger}$ value due to the degeneracy of the three two-ring flip processes.[17b] When the degeneracy is partially removed, as in **26**[59] two coalescence processes, one for the *o*-methoxy and one for the *o*-methyl group, with appreciably different $\Delta G_c^{\ddagger}$ values were observed.[15,17c,59] The two $\Delta G_c^{\ddagger}$ values were ascribed to the two diastereomeric two-ring flips, in spite of the fact that each process occurs by a correlated motion of the three rings. It is clear from this example that for system **4** with chemically different aryl

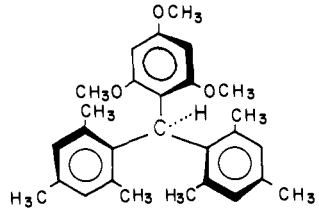

26

groups the two-ring flip mechanism cannot exchange simultaneously diastereotopic groups on the three rings. Consequently, a single rotational mechanism cannot be monitored in the three rings and the occurrence of correlated rotation has to be supported by other, independent ways. Indeed, Mislow applied molecular mechanics calculations for this purpose.[17d,e]

Effect of Substituents on the Threshold Barriers. Importance of Steric Congestion. The identification of the three-ring flip as the threshold mechanism for rotation in the crowded triarylvinyl propellers studied in the present work raises four interrelated questions. First, what is the mechanistic significance of the different $\Delta G_c^{\ddagger}$ values for the different substrates, and are the barriers dependent on the conformation and the presence or the absence of axial symmetry of the X groups? Second, is the three-ring flip the preferred route for rotation in all the vinyl propellers or is it limited only to the enols **1** and **25** and to closely related molecules, and do other routes operate for other types (e.g., with two blades or less crowded) of vinyl propellers? Third, why is the three-ring flip the threshold mechanism for triarylvinyl propellers, whereas the two-ring flip is the threshold mechanism for the Ar_3Z propellers **3** and **4**? Fourth, can one separate enantiomeric or diastereomeric stable enols or their derivatives?

The propeller conformation is obviously lower in energy than the overall planar conformation, which resembles the transition state for the zero-ring flip, or from the conformation with three parallel rings, which resembles the transition state for the 3-ring flip. On steric grounds alone increase in the in-plane bulk of any one of the four double-bond substituents compared to an arbitrary standard should increase the energy of the planar form and the torsional angle of the aryl rings and correspondingly the ground-state energy. Contributions from secondary effects such as hydrogen bonding or steric attraction can also be important. This will be the main effect of the substituent X, although, with a multiatom X, steric inhibition to form the transition state may be envisioned. The transition-state interaction is between the three perpendicular flipping rings, and the "thicker" the rings, the higher will be the interaction and the rotational barrier.

A revealing comparison is therefore between the rotation barriers of **1** (18.4 kcal mol^{-1}) and **25** (16.2 kcal mol^{-1}). Hine discussed recently the relative bulks of 9-anthryl and mesityl.[60] He concluded that 9-anthryl is thinner since it contains only sp^2 carbons and "when it is perpendicular to a carbon–carbon double bond it will repel a group cis to it less than a mesityl group would". This situation is encountered in the transition state of the three-ring flip, which should therefore be less crowded for **25** than for **1**. An opposite situation should be expected for the transition states of the zero-ring flip that involve these two groups. The energy differences should, however, reflect also the ground-state differences of the two compounds. The X-ray data show that the main conformational difference between **1** and **25** is the larger torsional angle of the α-9-anthryl group of **25** compared with that for the α-mesityl group of **1**.[13] Consequently, a smaller geometrical change is required for the enantiomerization of **25** than that for **1**, and if this is also accompanied by a corresponding reduction in energy, the lower barrier for **25** reflects both ground-state and transition-state effects.

The sensitivity of the barriers to the location of the rings, which reflects the different α, β, $\alpha\beta'$, and $\beta\beta'$ ring interactions in the transition states is also shown by significant differences in $\Delta G_c^{\ddagger}$ values for the coalescence of the isomeric 2,2-dimesityl-1-phenylethenol and (*Z*)-1,2-dimesityl-2-phenylethenol or for the isomeric (*E*)- and (*Z*)-1,2-dimesityl-2-phenylvinyl acetates.[26]

A similar reduction of the rotational barrier on replacing a mesityl by a 9-anthryl group was also found for the threshold mechanism of a two-ring flip. The $\Delta G_c^{\ddagger}$ values for trimesitylmethane (**27**)[17b] and dimesityl-9-anthrylmethane (**28**)[17c] in $CHBr_3$

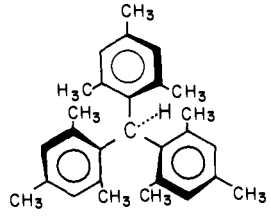

27

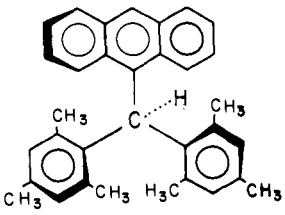

28

are 21.9 and 17.2 kcal mol^{-1}, respectively. Since the transition states mainly reflect interactions of two flipping mesityl groups for **1** and the flipping mesityl and 9-anthryl groups for **25**, the interpretation of the lower barrier is probably similar to that discussed above. However, the difference of 4.7 kcal mol^{-1} is larger than the $\Delta\Delta G_c^{\ddagger}$ difference of 2.2 kcal mol^{-1} for **1** and **25**. Hence both the $\Delta G_c^{\ddagger}$ and the $\Delta\Delta G_c^{\ddagger}$ values are higher for system **4**, X = H, than for system **2** when X is larger than H. Since the two-ring flip is the threshold mechanism, the energy of the three-ring flip in **27** and **28** is higher than the values reported above. Consequently, the difference in the barriers of the three-ring flip routes between systems **2** and **4** should be very appreciable.

These and other data offer a rationalization as to why the three-ring flip becomes the preferred enantiomerization route for the vinyl propellers. Mislow noted that the $\Delta G_c^{\ddagger}$ values for triarylboranes are a 3–5 kcal mol^{-1} lower than for the corresponding triarylmethanes.[17c] For example, $\Delta G_c^{\ddagger}$ for **22** (which is expected to be similar to that of trimesitylborane) and for dimesityl-9-anthrylborane **29** are 17.8 and 13.9 kcal mol^{-1}, respectively. This

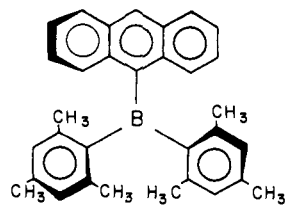

29

(59) Sabacky, M. J.; Johnson, S. M.; Martin, J. C.; Paul, I. C. *J. Am. Chem. Soc.* **1969**, *91*, 7542.

(60) Hine, J.; Skoglurd, M. J. *J. Org. Chem.* **1982**, *47*, 4758.

was partly attributed to the longer C–B bonds compared with the C–C bonds to the central carbon, which lead to a more open structure and to reduced steric congestion in both the ground and the transition states. Another factor is the somewhat smaller C–C–C angles compared with the C–B–C angles. Nonbonded interactions of X, which are absent for the boranes, may also affect the $\Delta G_c^{\ddagger}$ values. We note that the barriers are further reduced when the central atom becomes even larger: $\Delta G_c^{\ddagger}(Mes_3CH) > \Delta G_c^{\ddagger}(\mathbf{29}) > \Delta G_c^{\ddagger}(Mes_3P) > \Delta G_c^{\ddagger}(Mes_3As)$.[17c,61]

Several effects reduce the energy of the three-ring flip compared with the two-ring flips in crowded systems **2**. The angle between the β and the β' rings approaches 120° at least in the transition state. This is similar to the borane series except that the Ar–C(sp^2) bonds are shorter than in **27**. The angle between the α and the β rings is probably somewhat larger than 60° when X is small, but the α ring is one carbon removed in comparison with the situation in **4**. When the X substituent is a single atom, it is in the plane of the double bond, but when it is a multiatom group it may extend to other planes. Inspection of space-filling models reveals the following steric interactions in the ground and the transition states. In a geared flip process of the β and β' rings, or of the α and the β rings, the distances between nonbonded methyl groups on the two rings decrease. The β ring is therefore the most hindered ring in the transition state. The two-ring flip with the lowest energy depends on several interactions. If the nonflipping ring is the β ring its interaction with the flipping α ring is larger than with the flipping β' ring, since the smaller angles more than compensate for the larger distance, and the bumping of the *o*-methyl group into the ring is apparently larger in the latter case. The same unfavorable interaction also takes place when the α ring is nonflipping and the β ring is flipping. In these two latter cases a severe interaction with the X group in the planar part of the transition state takes place and in most cases the X–β'-ring interaction will be more pronounced than the X–α-ring interaction due to the different angles. The overall result is that the narrow angles beween pairs of cis substituents on the double bond are in large part responsible for the high steric interactions in the two-ring flip, making the three-ring flip the threshold process. In contrast, systems **3** and especially **4** can accommodate more easily the nonflipping ring in the transition state for the two-ring flip.

Viewed differently, the same steric interactions are also responsible for the ground-state structures. The higher the torsional angles in the most stable ground-state conformation, the higher is the energy to give the complete or partial planar arrangement of all or several of the groups in the zero-, one-, and two-ring flips. At the same time the three-ring flip is, at least for some of the rings, the least motion pathway, which is apparently associated with the lower activation energies.

This analysis suggests that the three-ring flip is not necessarily the universal threshold mechanism for all the vinyl propellers. Even within the more limited series of $Ar_2C{=}C(X)Ar$, the in-plane steric interaction of nonflipping rings can be reduced sufficiently so that a two-ring flip may become the threshold mechanism. Favorable conditions that should be fulfilled are reduction in the bulk of both X and the β ring. This should be reflected in the ground-state static structure and a system where the X-ray diffraction will show that at least one ring has a low torsional angle (e.g., 30°) may be a favored candidate for a two-ring flip. We have some preliminary indications that a two-ring flip in systems with the above characteristics do indeed occur.[26]

The above analysis also suggests systems for which optical resolution of enantiomers is feasible, i.e., system which will show atropisomerism. Attempted resolutions of **1** on optically active columns[62] had failed, which is not surprising in view of the rotational barriers of Tables VII and IX. The lower barrier for the "thinner" α-9-anthryl group and the higher barrier when X = OAc suggest that the thickness of one or more of the aryl groups should be appreciably increased in order to increase the barrier for the three-ring flip, while keeping the barrier for the two-ring flip high, either by increasing the bulk of X (i.e., when X = OAc) or by increase in the "wideness" of the rings, especially the β ring. Tentatively, compounds such as **30** where a 2,6-diisopropylphenyl

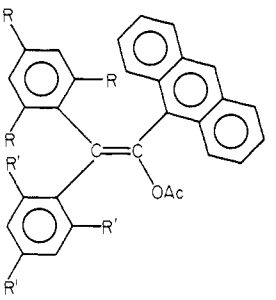

30, R = R′ = *i*-Pr
R = *i*-Pr; R′ = Me

or a 2,6-di-*tert*-butylphenyl ring replaces one or two of the mesityl group(s) of **1** and the third one is replaced by a 9-anthryl group will be likely candidates for optical resolution.

The $\Delta G_c^{\ddagger}$ barriers for different X groups follow the order $OCHMe_2 < Cl < OH < OAc$. Although the values were measured in different solvents, this should not affect this order since the average values for **1** in different solvents [18.1 ± 0.2 (Me_2SO), 18.4 ± 0.1 ($C_6D_5NO_2$) and 18.4 ± 0.1 (1,2,4-$C_6H_3Cl_3$)] are identical within the experimental error.

Since all the four double-bond substituents are inductively electron withdrawing and resonance interactions between the substituents and the twisted rings are low, electronic effects cannot account for this order. From the above discussion, we expect that the $\Delta G_c^{\ddagger}$ values will mainly reflect the steric bulk of X. The absence of a correlation between $\Delta G_c^{\ddagger}$ and the gross steric bulk is not surprising since OH, $OCHMe_2$, and OAc are multiatom groups and their bulk at the reaction site depends on their conformations in relation to the α and β' rings and on the barrier for interconversion of various conformations.

The simpler case is when X = Cl since chlorine is bulkier than OH if the C–O–H angle is taken into account. Consequently, the torsional angles of neighboring rings should increase, hence raising the ground-state energy and reducing the barriers, compared with OH, as was indeed observed. For OH, $OCHMe_2$, and OCOMe, several conformations are possible and designations specifying the relationship between the substituents around the various bonds are required. The first designation is syn and anti (s-syn and s-anti) and relates to the arrangement of substituents around the C–O bond. The only two extreme conformations for **1** are **1**-*syn* and **1**-*anti*. With $OCOCH_3$, further rotation around the O–CO bond can lead to additional conformations. If the methyl group is in the double-bond plane, it can either be in a syn or an anti relationship to the C=O bond, giving altogether four conformers, e.g., **18**-*syn,anti*. However, the methyl group

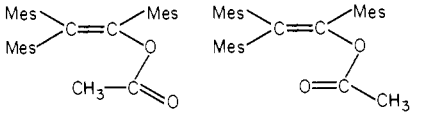

18-*syn,syn*

18-*syn,anti*

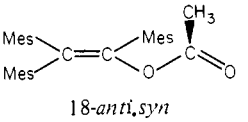

18-*anti,syn*

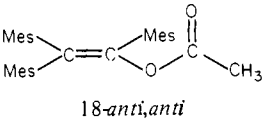

18-*anti,anti*

and the C=C bond are not necessarily in the same plane. For example, if in **18**-*syn,syn* Me and C=C are not eclipsed, they could be staggered. Due to the chirality of the propeller residue, methyl groups above and below the C=C plane become diastereotopic, giving rise to diastereomeric acetates. One conformer

(61) Bellamy, A. J.; Gould, R. O.; Walkinshaw, M. D. *J. Chem. Soc., Perkin Trans. 2* **1981**, 1099.

(62) These experiments were conducted in the laboratories of Professors E. Gil-Av and W. A. Pirkle.

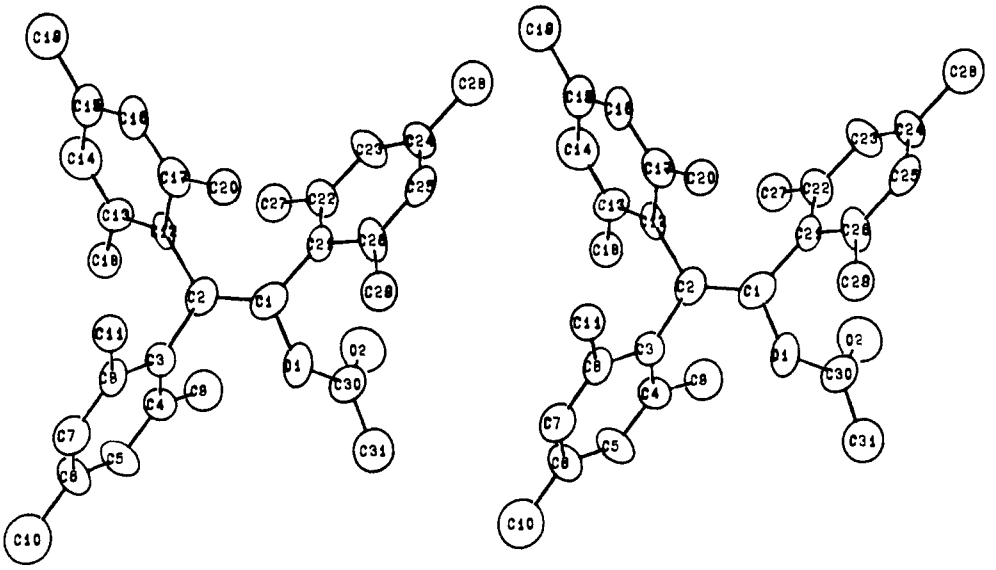

Figure 9. Stereoscopic view and numbering scheme of **18**.

of the **18**-*anti,syn* is shown above.

The syn and the anti designations for **19** relate again to the relationship between the double bond and the isopropyl group.

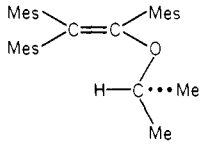

19-*syn-eclipsed-H*

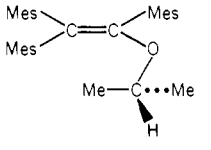

19-*syn-eclipsed-Me*

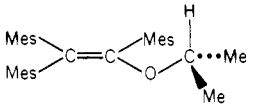

19-*anti-eclipsed-H*

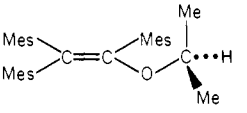

19-*anti-eclipsed-Me*

In two extreme conformations either the hydrogen or the methyl may be eclipsed with the double bond, and this is given specifically in the name, e.g., **19**-*anti-eclipsed-Me*. Staggered conformations are also possible.

In general, the syn conformations should lead mainly to interaction between X and the β' ring, whereas the anti conformation will lead mainly to an X-α-ring interaction.

So that information on the importance of the various conformations of $Mes_2C{=}C(X)Mes$ systems could be obtained, low-temperature ^1H NMR of **1**, **18**, and **19** and X-ray diffraction data for **18** were obtained.

From X-ray data[13] the conformation of **1** in the solid state is **1**-*syn*. From studies of the solvent dependence of the chemical shift of the OH group and analogies with other systems, **1**-*syn* is the preferred conformation in aprotic nonpolar solvents such as $CDCl_3$, but an anti-clinal conformation predominates in hydrogen-bonding accepting solvents such as Me_2SO. In solvents with intermediate character such as acetone, a mixture of the two conformers is indicated.[26] Since the rotational barriers are practically identical in 1,2,4-trichlorobenzene where the conformation is presumably **1**-*syn*, in $C_6D_5NO_2$ where both conformations probably exist, and in DMSO where the anti-clinal conformation predominates, the barriers are apparently unaffected by the OH conformation.

When a solution of **1** in CD_3COCD_3—a solvent where both conformers are probably present—is cooled to 213 K, no broadening of the sharp OH signal was detected. Consequently, any process leading from **1**-*syn* to **1**-*anti*, which may be either a rotation around the C–O bond or oxygen inversion, is rapid on the NMR time scale, with $\Delta G_c^{\ddagger} < 10$ kcal mol^{-1}. The "rotation" of the OH group occurs faster than the flip of the rings, and this process, which should increase the "effective" volume of the OH group, apparently does not change the rotational barrier, since even the rotating OH group is small, at least when compared with chlorine.

The isopropoxy derivative **19** has the lowest rotational barrier. According to our explanation this should reflect an increase in the ground-state energy due to steric interaction of X and the aryl groups if the isopropoxy group occupies a syn conformation. There are theoretical calculations and experimental observations which suggest that the syn conformation of vinyl ethers is important or predominant,[24,63] but it is doubtful whether these results are applicable to crowded systems such as **19**. Since X-ray data are not available, we tried to gain conformational information from the NMR spectrum. Comparison of the ^1H NMR spectrum of **19** and methyl trimesitylvinyl ether ($Mes_2C{=}C(OMe)Mes$) in $CDCl_3$ showed that all the protons of **19**, except for the three *p*-Me groups and the *o*-Me groups of the β' ring, are more deshielded by an average of 0.04 ppm. This change is too small for deriving reliable conformational information and the conformation of **19** is presently unknown. However, it is known that the barrier to any conformational change, if any, is very low since when a solution of **19** in $CDCl_3$ is cooled to 213 K, no splitting of the signals, which is expected when several conformations are present (see below), was observed.

Conformational Changes in Trimesitylvinyl Acetate. In contrast with **19**, the $\Delta G_c^{\ddagger}$ values for **1** and its acetate **18** differ by only 0.6 kcal mol^{-1}. This is reasonable if the bulk of the acetate group is directed away from the β' ring, i.e., if the acetate group occupies one of the anti conformations. In order to answer this question and to find out whether derivatives of **1** still retain the propeller conformation, the structure of **18** was determined by X-ray crystallography. The structure is drawn in Figure 9 and important features are given in Table XI. The following features are of interest: (a) The structure is that of a vinyl propeller. (b) The acetate group is in an anti,anti conformation where the carbonyl plane is twisted by 54° from the ideally planar conformation. (c) The double bond is slightly twisted with a twist angle of 10° between the planes defined by C_α and the C_α substituents and C_β and its substituents. (d) The torsional angles of the mesityl groups (α 59°, β 57°, β' 64°) are similar to those found for **1**.[13]

The preference for the twisted anti,anti conformation can be ascribed to two reasons. First, the steric effect of the OH group is small, and any increase in ground-state energy due to the syn

(63) For recent references, see: (a) Fischer, P. In "The Chemistry of Functional Groups, Supplement E."; Patai, S., Ed.; Wiley-Interscience: New York, 1980; Part 2, Chapter 17. (b) Mersh, J. D.; Saunders, J. K. M. *Tetrahedron Lett.* **1981**, *22*, 4029. (c) Hine, J.; Linden, S.-M. *J. Org. Chem.* **1981**, *46*, 1635.

Table XI. Relevant Crystallographic Data for 18[a,b]

bond	length, Å	angle	deg	angle	deg
C(1)-C(2)	1.33 (1)	C(2)-C(1)-C(21)	128 (1)	C(21)-C(26)-C(25)	118 (1)
C(1)-C(21)	1.51 (1)	C(2)-C(1)-O(1)	117 (1)	C(21)-C(26)-C(29)	123 (1)
C(1)-O(1)	1.39 (1)	C(21)-C(1)-O(1)	114 (1)	C(25)-C(26)-C(29)	118 (1)
C(2)-C(3)	1.48 (1)	C(1)-C(2)-C(3)	119 (1)	C(1)-O(1)-C(30)	121 (1)
C(2)-C(12)	1.48 (1)	C(1)-C(2)-C(12)	124 (1)	O(1)-C(30)-O(2)	122 (1)
C(21)-C(22)	1.40 (1)	C(3)-C(2)-C(12)	117 (1)	O(1)-C(30)-C(31)	110 (1)
C(21)-C(26)	1.42 (1)	C(1)-C(21)-C(22)	122 (1)	O(2)-C(30)-C(31)	128 (1)
C(22)-C(23)	1.37 (1)	C(1)-C(21)-C(26)	118 (1)		
C(22)-C(27)	1.50 (1)	C(22)-C(21)-C(26)	119 (1)	plane (1)-plane (2)[c]	10 (1)
C(23)-C(24)	1.37 (2)	C(21)-C(22)-C(23)	118 (1)	α ring-plane (1)[c]	59 (1)
C(24)-C(25)	1.38 (2)	C(21)-C(22)-C(27)	121 (1)	β ring-plane (2)[c]	57 (1)
C(24)-C(28)	1.51 (1)	C(23)-C(22)-C(27)	120 (1)	β' ring-plane (2)[c]	64 (1)
C(25)-C(26)	1.37 (2)	C(22)-C(23)-C(24)	124 (1)	plane (1)-OAc[c,d]	54 (1)
C(26)-C(29)	1.50 (1)	C(23)-C(24)-C(25)	116 (1)		
O(1)-C(30)	1.38 (1)	C(23)-C(24)-C(28)	122 (1)		
C(30)-O(2)	1.19 (1)	C(25)-C(24)-C(28)	122 (1)		
C(30)-C(31)	1.45 (1)	C(24)-C(25)-C(26)	123 (1)		

[a] Bond lengths and angles are demonstrated only for the α ring. For other data see supplementary tables. [b] Deviations in the least significant digits are given in parentheses. [c] Plane(1) is defined by C(21)C(1)O(1) and plane(2) by C(12)C(2)C(3). [d] The plane of the acetate group is defined by C(30)O(1)O(2)C(31).

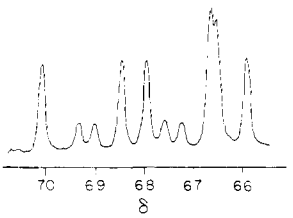

Figure 10. ^{1}H 300-MHz NMR spectrum of the aromatic region of **18** in $CDCl_3$ at 212 K.

conformation can be compensated by the energy gain of the internal OH–π(Ar) hydrogen bond in **1**-*syn*. Such hydrogen bonding is impossible for **18** and the less crowded anti conformations will be preferred. Of the two anti conformations, **18**-*anti,anti* seems to be less sterically hindered, and the twist of the carbonyl group from the plane of the double bond probably reduces further the steric interactions. Second, crystal-packing effects may also be responsible for obtaining this structure in the solid state.

When a solution of **18** in $CDCl_3$ was cooled, several signals broadened and finally split. At 212 K the NMR at the methyl region, which includes both the mesityl and the acetoxy methyl groups, showed 10 signals of high intensity and eight signals of lower intensity. Six high-intensity and four low-intensity signals were observed in the aromatic region (Table XII and Figure 10). It is therefore clear that two conformers (with few overlapping signals) exist at low temperature and that the room temperature spectrum is due to averaging of the signals of these conformers by rapid interconversion on the NMR time scale. Most of the signals belonging to each conformer were distinguished by comparing the spectra at 212 and 298 K, by using the saturation transfer technique to all the signals, and by integration since one conformer is in large excess. By averaging the intensities of all the signals for each conformer, the conformer ratio was found to be 3.4:1; i.e., ΔG° = 0.52 kcal mol^{-1} at 212 K. Similarly, the NMR spectrum of the acetate **21** shows the presence of two conformers in a 4:1 ratio.

Analogy with the solid-state conformation suggests that both conformers have an anti configuration around the C–O bond. If this is indeed the case, this is consistent with the higher rotational barrier, compared with that for **1**, as discussed above. From space-filling models the least crowded conformations are indeed with an anti arrangement around the C–O bond. However, the two conformers may either be **18**-*anti,anti* and **18**-*anti,syn* or two diastereomers of **18**-*anti,anti* that differ by the relative position of the methyl group of the acetate, which can be either "up" or "down" in respect to the double bond. We are unable to distinguish at present between these alternatives.

Table XII. Chemical Shifts (ppm) for the Two Conformers of 18 in $CDCl_3$ at 212 K

major conformer	minor conformer
1.74 (Me)	1.75 (Me)(sh)
1.80 (Me)	1.80 (2 Me)
1.90 (Me)	
1.94 (Me)	1.98 (Me)
2.05 (Me)	2.07 (Me)
2.16 (Me)	2.16 (Me)[a]
2.22 (Me)	2.24 (2 Me)
2.28 (Me)	
2.32 (Me)	2.36 (Me)
2.47 (Me)	2.55 (Me)
6.59 (Mes H)	6.65 (Mes H)[a]
6.65 (Mes H)	6.66 (Mes H)[a]
6.66 (Mes H)	6.72 (Mes H)
6.79 (Mes H)	6.76 (Mes H)
6.84 (Mes H)	6.90 (Mes H)
7.01 (Mes H)	6.93 (Mes H)

[a] Peaks obscured by those of the major conformer.

The interconversion of the two conformers was monitored in $CDCl_3$ by following the coalescence processes in the temperature range 221–269 K. Since the populations of the two species are different, we used the total line-shape analysis method in order to obtain the $\Delta G_c^\ddagger$ values,[52] which were found to be similar for all the processes. The $\Delta G_c^\ddagger$ values, starting from the stable conformer, are 12.4 and 11.8 kcal mol^{-1} for the forward and the reverse exchange, respectively. If the process is an **18**-*anti,anti* ⇌ **18**-*anti,syn* interconversion it is probably a rotation around the C–CO single bond. We believe that the steric hindrance in the system is partly responsible to the barrier height, since for less hindered triarylvinyl acetates we were unable so far to see splitting of the signals, due to the presence of two conformers, at low temperatures.[26]

It should be emphasized that the large difference between the above $\Delta G_c^\ddagger$ values and the $\Delta G_c^\ddagger$ value of 19 kcal mol^{-1} for the correlated rotation indicate that the rotations of the acetate group and the rings are not coupled. In spite of the inherent nonconical symmetry of the acetate group, its fast free rotation makes it effectively symmetrically conical on the average at the stage when the mesityl groups undergo the flip process.

Finally, an interesting feature of the NMR data is that an acetate group that is remote from part of the molecule, at least from the α ring, still affects the chemical shift of almost all the protons as shown by the distinct spectra of the two conformers. The anisotropy of the carbonyl group may contribute to this, but it is likely that the main reason is that in a congested molecule such as **18** any small change in the torsional angle of one ring will be reflected by some motion of the other rings. Consequently,

in the ground state of the substituted derivatives the torsional angles of the three rings are different either for different X groups or even for different conformers of the same X group.

Conclusions. Crowded $Mes_2C{=}C(X)Mes$ and related systems exist in the solid state and in solution in a chiral propeller conformation. The threshold rotational mechanism which leads to enantiomerization by helicity reversal is a correlated rotation of the rings via a three-ring flip. The $\Delta G_c^{\ddagger}$ values for the enantiomerization depend on the "width" of the aryl rings and on the nature of the substituent X. Nonconical substituents such as OAc can exist in two distinct conformations at low temperature, but the threshold energy for their interconversion is well below the value for the three-ring flip.

Experimental Section

General Methods. Melting points are uncorrected. UV spectra were measured with a Gilford 2400-S spectrophotometer, and infrared spectra were taken with a Perkin-Elmer 157 G spectrometer. The X-ray diffraction of a single crystal of **18** was measured on a PW 1100 Philips four-circle computer-controlled diffractometer equipped with a five-focus Mo X-ray tube and a graphite crystal monochromator in the incident beam.[64]

^1H and ^{13}C NMR spectra were recorded on a Bruker WH-300 pulsed FT spectrometer operating at 300.133 and 75.46 MHz for ^1H and ^{13}C, respectively. The ^1H NMR samples were prepared by dissolving ca. 20 mg of the compound in 0.5 mL of solvent. The field/frequency regulations were maintained by locking to the solvent's deuterium. The free-induction decay signals were digitized and accumulated on an Aspect 2000 computer (32K). In the DNMR measurements, ^1H NMR spectra were recorded on a Varian HA-100 or on a Bruker WH-300 spectrometer, equipped with variable-temperature accessories. Temperature measurements were based on the chemical-shift separation of the protons of an ethylene glycol sample, and utilization of the temperature-shift correlation of Van Geet.[65] Temperatures are considered to be accurate to ±2 °C for various sets of measurements and to ±0.5 °C within a given single series of measurements. Saturation of the NMR signals was avoided. The HA-100 spectra were calibrated by using the difference in frequency between the local signal and the pen position (DIFF 1 of the signal monitor) as measured on the V-4315 signal counter. The $\Delta G_c^{\ddagger}$ values were determined from the exchange rate constant at T_c. Saturation transfer studies were carried out with a Bruker WH-300 spectrometer. Most of the irradiations were carried out at room temperature, but in the compounds of higher rotational barrier (e.g., **1**, **18**) it was necessary to heat the sample to 50 °C in order to observe the effect.

Important features of the mass spectra of **1**, **13**, **14**, **15**, **16**, **18**, **20**, and **25** are given in ref 12b.

Solvents and Materials. Tetrahydrofuran (THF) was distilled from sodium benzophenone ketyl under nitrogen immediately before use. Ether and toluene were distilled from sodium, and pyridine was distilled from KOH. In each case only the middle fraction was collected and stored over 4-Å molecular sieves. The solvents for the chromatography were purified by distillation. The deuterated NMR solvents were the best commercial samples and were used without further purification.

Trimesitylethenol was prepared by a modification of Fuson's method,[9c] which is described below for the synthesis of the deuterated derivative **13**. The preparation of the *tert*-butyl analogue will be given elsewhere.[26] **Trimesitylvinyl acetate** was obtained by reaction of the enol **1** with acetic anhydride and pyridine according to Fuson.[9c]

Mesitylene-*methyl*-d_9. Mesitylene was deuterated in the three methyl groups by exchanging it three consecutive times with 99.5% D Me_2SO-d_6/NaH at 100 °C according to the literature procedure.[38a] The sample used for the further synthesis was 98.4% deuterated in the methyl groups according to its 300-MHz ^1H NMR spectrum.

1-(2,4,6-Tri(methyl-d_3)phenyl)-2,2-dimesitylethenol (13). (a) **2-Bromomesitylene-*methyl*-d_9.** Mesitylene-*methyl*-d_9 was brominated according to the literature procedure for the unlabeled compound.[38b] Starting from mesitylene-d_9 (6 mL) 2-bromomesitylene-*methyl*-d_9 (98.4% deuterated) (2.8 mL, 44%) was obtained. No impurities could be detected by NMR or by gas chromatography.

(b) To a cooled solution of dimesitylacetic acid[12b] (0.5 g, 1.7 mM) and thionyl chloride (0.125 mL, 1.7 mM) in dry toluene (12.5 mL) was added dry pyridine (0.025 mL, 0.3 mM), and the mixture was refluxed for 2 h, the solution was decanted from the precipitated pyridinium hydrochloride, the toluene was evaporated, and the resulting dimesityl ketene was dissolved in dry THF (20 mL). The solution was added dropwise during 15 min to a solution of a Grignard reagent prepared from 2-bromomesitylene-*methyl*-d_9 (0.68 g, 3.3 mM) and magnesium (86 mg, 3.6 mM) in dry THF (20 mL). After the addition was completed, the mixture was refluxed for 2.5 h. The deep red mixture was poured on a saturated solution of NH_4Cl, the phases were separated, and the aqueous phase was extracted with ether (2 × 50 mL). The combined organic phase was dried (Na_2SO_4) and evaporated, yielding a solid (350 mg, 51%), which was purified by dissolving it in hot ethanol (10 mL) and cooling. The product, which was pure according to the NMR, was recrystallized from ethanol, giving crystals of pure **13**, mp 158 °C.

1-(2,6-Dimethylphenyl)-2,2-dimesitylethenol (14). To a Grignard reagent that was prepared from 1-bromo-2,6-dimethylbenzene (5.81 g, 28.3 mmol) and magnesium (0.68 g, 28 mmol) in dry THF (50 mL) was added dimesityl ketene (3.75 g, 13.5 mmol) in dry THF (50 mL) dropwise during 30 min. The mixture was poured into a 10% aqueous NH_4Cl solution (100 mL), extracted with ether (2 × 50 mL), and dried, and the solvent was evaporated. The resulting orange oil was crystallized by dissolving it in warm ethanol and addition of petroleum ether. The yellow solid, mp 137–140 °C (1.6 g, 31%), was recrystallized from ethanol–petroleum ether giving 1.4 g (27%) of white crystals of **14**: mp 143 °C; ν_{max} (Nujol) 3540, 3460 (OH), 1600 (C=C) cm^{-1}. λ_{max}(MeOH): 238 nm sh (25700), 280 nm (19200). Anal. Calcd for $C_{31}H_{38}O$: C, 87.45; H, 8.39. Found: C, 87.64; H, 8.31.

Isopropyl Trimesitylvinyl Ether (19). To a solution of **1** (240 mg, 0.6 mM) and benzyltriethylammonium chloride (70 mg, 31 mM) in 2-bromopropane (20 mL) was added a solution of 50% aqueous NaOH (10 mL), and the mixture was stirred overnight under reflux. Ether (20 mL) was then added, the phases were separated, and the organic phase was washed with water (3 × 10 mL) and evaporated. Recrystallization of the residue from ethanol (10 mL) gave colorless crystals of the ether **19**: mp 168 °C (210 mg, 80%); ν_{max} (Nujol) 1610 (C=C), 1585 cm^{-1}; λ_{max} (MeOH) 223 nm (ε 34400), 283 nm (15400). Anal. Calcd for $C_{34}H_{32}O$: C, 87.52; H, 9.15. Found: C, 87.37; H, 9.30.

Trimesitylvinyl Chloride (20). To a solution of **1** (0.5 g, 1.26 mmol) in dry toluene (25 mL) were added thionyl chloride (4 mL, 54.4 mmol) and dry pyridine (0.1 mL, 1.2 mmol). The yellow mixture was stirred for 5 h at room temperature, after which the reaction was complete by NMR and TLC. The mixture was decanted from the pyridinium hydrochloride and evaporated. Three recrystallizations from petroleum ether (40–60 °C) afforded colorless crystals of **19** (340 mg, 65%): mp 188–189 °C; ν_{max} (Nujol) 1610 (C=C) cm^{-1}; λ_{max} (MeOH) 228 nm (ε 21600), 240 nm sh (19700), 278 nm (13100). Anal. Calcd for $C_{29}H_{33}Cl$: C, 83.52; H, 7.98; Cl, 8.50. Found: C, 83.26; H, 8.21; Cl, 8.96.

1-(2,6-Dimethylphenyl)-2,2-dimesitylvinyl Acetate (21). A mixture of **14** (200 mg, 0.5 mmol), acetic anhydride (1.5 mL), and pyridine (0.5 mL) was refluxed for 5 h. The mixture was poured into ice water, and the solid obtained was recrystallized from ethanol, giving 160 mg (75%) of **21**: mp 158–159 °C; ν_{max} (Nujol) 1745 (AcO), 1610 (C=C) cm^{-1}; λ_{max} (MeOH) 240 nm sh (ε 22900), 274 nm (13100). Anal. Calcd for $C_{28}H_{32}O$: C, 84.47; H, 8.03. Found: C, 84.70; H, 7.88.

1-(9-Anthryl)-2,2-dimesitylethenol (25). To a Grignard reagent that was prepared from 9-bromoanthracene (2.0 g, 7.8 mmol) in a mixture of ether (30 mL) and dry toluene (15 mL) was added dimesityl ketene (2.2 g, 7.7 mmol) in ether (30 mL) during 15 min. The mixture was refluxed overnight, poured into ice (100 g) containing concentrated HCl (5 mL), the phases were separated, and the aqueous phase was extracted with chloroform (3 × 50 mL). The combined organic phase was dried (Na_2SO_4), and the solvent was evaporated. The residue was chromatographed on dry silica column (160 g) with petroleum ether 40–60 °C as the eluent. Anthracene (1.21 g), **25** (0.50 g), and an unidentified compound (1.36 g) were eluted in this order. Crystallization from ether gave yellow crystals (320 mg, 8.7%) of the enol etherate **25**·$C_2H_5OC_2H_5$ as shown by NMR, mp 236–237 °C. Further crystallization from petroleum ether gave pure **25**: mp 246 °C; ν_{max} (Nujol) 3500 (OH), 1610 (C=C) cm^{-1}; λ_{max} (MeOH) 250 nm (ε 100400), 397 nm (9500); mass spectrum (high resolution) calcd 456.2408, found 456.2453. Anal. Calcd for $C_{34}H_{32}O$: C, 89.43; H, 7.06. Found: C, 88.13; H, 6.86.

Acknowledgment. We are indebted to Professors K. Mislow, R. Glaser, D. Gust, and M. Öki and to Drs. M. Kaftory and D. Kost for helpful discussions, correspondence, and comments, to Dr. S. Cohen for the X-ray diffraction, to Dr. S. Blum for the microanalyses, and to Professors W. A. Pirkle and E. Gil-Av for an attempted separation of **1** This work was supported by a grant from the United States-Israel Binational Science Foundation

(64) The material crystallized in the monoclinic $P2_1/c$ space group with four molecules in a cell of dimensions a = 13.910 Å, b = 11.599 Å, c = 16.551 Å, and β = 99.50°. The R factor is 0.131. A comprehensive list of the coordinates and bond lengths and angles is given in the supplementary tables S1–S3.

(65) Van Geet, A. L. *Anal. Chem.* **1968**, *40*, 2227; **1970**, *42*, 679.

(BSF), Jerusalem, Israel, to which we are grateful.

Registry No. 1, 26905-20-4; **13**, 87871-28-1; **14**, 87871-29-2; **18**, 38659-55-1; **19**, 87871-30-5; **20**, 87871-31-6; **25**, 80062-28-8; 2-bromomesitylene-*methyl*-d_9, 87871-32-7; dimesitylacetic acid, 5740-42-1; dimesityl ketene, 87871-33-8; mesitylene-*methyl*-d_9, 15690-50-3; 1-bromo-2,6-dimethylbenzene, 576-22-7; 9-bromoanthracene, 1564-64-3.

Supplementary Material Available: Tables S1-S3 giving the crystallographic data for compound **18** (3 pages). Ordering information is given on any current masthead page.

Highly Specific Reciprocal Methyl/Hydrogen Transfer Reactions Preceding Some Unimolecular Dissociations of Crowded Enol Cation Radicals in the Gas Phase as Examples for Conformationally Controlled Processes

Silvio E. Biali,[1a] Gisbert Depke,[1b] Zvi Rappoport,*[1a] and Helmut Schwarz*[1b]

Contribution from the Department of Organic Chemistry, The Hebrew University of Jerusalem, Jerusalem 91904, Israel, and the Institut für Organische Chemie der Technischen Universität Berlin, D1000 Berlin 12, West Germany. *Received March 22, 1983*

Abstract: The molecular ions of α-(*o*-methyl)-substituted triarylethenols contain in their metastable ion (MI) mass spectra signals for radical losses that are derived from highly site specific reciprocal CH_3/H migrations. The study of analogues, including some deuterium-labeled isotopomers, reveals the following unusual features: The ortho position of the α-aryl ring is the migration origin, and the ipso position of the β-ring (cis to it) is the terminus of the formal [1,5]-CH_3 migration. The hydrogen transferred back to the α-ring stems exclusively from the migrating CH_3 group. Other methyl rearrangements, from the β- to the α-ring or between the β- and the β'-rings, resulting in the eventual loss of a radical were not observed. No evidence was obtained for the operation of hydrogen scrambling processes. For the overall reaction, i.e., CH_3/H transfer and radical loss, a kinetic isotope effect is not operative. The rearrangement is facilitated by the proximity of the migration origin and terminus in the propeller conformation of the crowded enols. The stereochemical and electronic properties of the C_β-aryl groups exert a directing influence on the direction of the CH_3 transfer. Steric and electronic effects in the products generated apparently determine the detailed course of the reaction in that the elimination of the β-aryl ring together with the transferred "CH_2" unit as a benzyl-type radical results exclusively in the generation of an α-aryl-substituted vinyl cation **20**, whereas a similar elimination of the α-aryl ring will generate the less stable isomeric ion **24**. When the cation resulting from the rearrangement is unstable, e.g., that obtained from the substituted indene **32**, the reciprocal CH_3/H migration followed by radical loss is of minor importance.

The gas phase chemistry of ionized keto/enol forms is a subject of very intense current research activity.[2] Whereas the thermodynamic and kinetic stabilities of most simple enols are quite low in comparison to their tautomeric keto forms,[3,4] the opposite usually holds when their ions are generated in the gas phase. MO calculations[5] and thermochemical studies demonstrate[6] that simple enol cation radicals are substantially more stable than their corresponding keto forms. Moreover, collisional activation (CA) mass spectrometric measurements reveal the existence of stable noninterconverting keto/enol ions, which must be separated by substantial energy barriers.[7] For decomposing ions it was shown that ionized ketones dissociate directly to closed-shell ions, in distinct contrast to the more complicated unimolecular pathways of enol ions. Some enol ions isomerize to the keto ions prior to dissociation, and others are known to rearrange to reactive intermediates of unusual structural properties before decomposing.[5]

Crowded enols differ in many respects from their more simple analogues. For example, ketone **1** is *less* stable than the enol form **3** by 0.6-1.1 kcal mol^{-1}, whereas **2**, following qualitatively the general trend of stability order, is more stable than **4** by 0.5-1.0 kcal mol^{-1}.[2a] For the corresponding ions it was observed that $\mathbf{3}^{+\cdot}$ is more stable than $\mathbf{1}^{+\cdot}$ by 14.4-14.9 kcal mol^{-1},[2a] in line with data for other keto/enol ions, where the ionized enol is more stable by 14-31 kcal mol^{-1}.[4b,6] Surprisingly, the ΔH°_f values for $\mathbf{2}^{+\cdot}$ and $\mathbf{4}^{+\cdot}$ are almost identical.[2a] However, the ionization of **2** and **4** does not lead to a common ion structure since the CA mass spectra

(1) (a) Hebrew University. (b) Technische Universität Berlin.

(2) For a quite comprehensive compilation of more recent references see: (a) Biali, S. E.; Lifshitz, C.; Rappoport, Z.; Karni, M.; Mandelbaum, A. *J. Am. Chem. Soc.* **1981**, *103*, 2896. (b) Schwarz, H. *Nachr. Chem., Tech. Lab.* **1978**, *26*, 792.

(3) (a) Hart, H. *Chem. Rev.* **1979**, *79*, 515. (b) Hart, H.; Sasaoka, M. *J. Chem. Educ.* **1980**, *57*, 685. (c) Tolluec, J. *Adv. Phys. Org. Chem.* **1982**, *18*, 1.

(4) For the preparation and spectroscopic study of the simplest enol, i.e., vinyl alcohol both in solution and in the gas phase, see: (a) Saito, S. *Chem. Phys. Lett.* **1976**, *42*, 399. (b) Holmes, J. L.; Lossing, F. P. *J. Am. Chem. Soc.* **1982**, *104*, 2648. (c) Capon, B.; Siddhantar, A. K. *Tetrahedron Lett.* **1982**, 3199. (d) Capon, B.; Zucco, C. *J. Am. Chem. Soc.* **1982**, *104*, 7567.

(5) (a) Bouma, W. J.; MacLeod, J. K.; Radom, L. *J. Am. Chem. Soc.* **1979**, *101*, 5540. (b) Bouma, W. J.; MacLeod, J. K.; Radom, L. *Ibid.* **1980**, *102*, 2246. (c) Hoppilliard, Y.; Bouchoux, G.; Jaudon, P. *Nouv. J. Chim.* **1982**, *6*, 43. (d) Frenking, G.; Heinrich, N.; Schmidt, J.; Schwarz, H. *Z. Naturforsch., B: Anorg. Chem., Org. Chem.* **1982**, *37B*, 1597. (e) Apeloig, Y.; Ciommer, B.; Frenking, G.; Karni, M.; Meyn, S.; Schmidt, J.; Schwarz, H., unpublished experiments.

(6) (a) Holmes, J. L.; Terlouw, J. K.; Lossing, F. P. *J. Phys. Chem.* **1976**, *80*, 2860. (b) Holmes, J. L.; Lossing, F. P. *J. Am. Chem. Soc.* **1980**, *102*, 1591.

(7) (a) Beynon, J. H.; Caprioli, R. M.; Cooks, R. G. *Org. Mass Spectrom.* **1974**, *9*, 1. (b) Van de Sande, C. C.; McLafferty, F. W. *J. Am. Chem. Soc.* **1975**, *97*, 4613. (c) Levsen, K.; Schwarz, H. *J. Chem. Soc., Perkin Trans. 2* **1976**, 1231. (d) McAdoo, D. J.; Witiak, D. N.; McLafferty, F. W.; Dill, J. D. *J. Am. Chem. Soc.* **1978**, *100*, 6639. (e) Schwarz, H.; Williams, D. H.; Wesdemiotis, C. *Ibid.* **1978**, *100*, 7052. (f) Schwarz, H.; Wesdemiotis, C. *Org. Mass Spectrom.* **1979**, *14*, 25. (g) Hemberger, P. H.; Kleingeld, J. C.; Levsen, K.; Mainzer, A.; Mandelbaum, A.; Nibbering, N. M. M., Schwarz, H.; Weber, R.; Weisz, A.; Wesdemiotis, C. *J. Am. Chem. Soc.* **1980**, *102*, 3736. (h) Maquestiau, A.; Flammang, R.; Glish, G. L.; Laramée, J. A.; Cooks, R. G. *Org. Mass Spectrom.* **1980**, *15*, 131. (i) Vajda, J. H.; Harrison, A. G.; Hirota, A.; McLafferty, F. W. *J. Am. Chem. Soc.* **1981**, *103*, 36. (j) For a review see: Levsen, K.; Schwarz, H. *Q. Rev. Mass Spectrom.* **1983**, 77.

0002-7863/84/1506-0496$01.50/0